Deposition of Vertically Aligned High Aspect Ratio Zinc Oxide Nanorods for UV and Gas Sensing Applications

By

M. Zafar Khan   Regn. No. NUST201304986BSCME99213F

Dawar Ali   Regn. No. NUST201305511BSCME99213F

Jawad Asif   Regn. No. NUST201306047BSCME99213F

School of Chemical and Materials Engineering (SCME)

National University of Sciences and Technology (NUST)

2017

Deposition of Vertically Aligned High Aspect Ratio Zinc Oxide Nanorods for UV and Gas Sensing Applications

M. Zafar Khan   **Regn. No. NUST201304986BSCME99213F**

Dawar Ali   **Regn. No. NUST201305511BSCME99213F**

Jawad Asif   **Regn. No. NUST201306047BSCME99213F**

This report is submitted as a FYP thesis in partial fulfillment of the requirement for the degree of

(BE in Materials Engineering)

Supervisor: Dr. Sofia Javed

Department of Materials Engineering

School of Chemical and Materials Engineering

National University of Sciences and Technology

June, 2017

Certificate

This is to certify that work in this thesis has been carried out by **Mr. Dawar Ali, Mr. Jawad Asif, Mr. Muhammad Zafar Khan** and completed under my supervision in Nano-synthesis laboratory, school of chemical and materials engineering, National University of Sciences and Technology, H-12, Islamabad, Pakistan.

Supervisor**: Dr. Sofia Javed**

Department of Materials Engineering
School of Chemical & Materials
Engineering,
National University of Sciences and
Technology, Islamabad

Co-supervisor**: Dr. Muhammad Mujahid**

Department of Materials Engineering
School of Chemical & Materials
Engineering,
National University of Sciences and
Technology, Islamabad

Submitted through:

_____

HoD**: Dr. Umair Manzoor**

Department of Materials Engineering
School of Chemical & Materials
Engineering,
National University of Sciences and
Technology, Islamabad

_____

Dean**: Dr. Muhammad Mujahid**

Department of Materials Engineering
School of Chemical & Materials
Engineering,
National University of Sciences and
Technology, Islamabad

Dedication

This work is dedicated to all those who carve a path for themselves despite sheer hardships and opposition. This work is symbol of courage and commitment for those who feel exhausted and loose hope. This work is dedicated to loving parents and honest friends who believe in you.

Acknowledgment

Abstract

The aim of this thesis is to optimize and evaluate the commonly used synthesis routes in order to achieve the desired ZnO nanorod morphology, and to investigate the variation in gas detection properties under the effect of UV light.

In the initial parts, basic information relating to the gas sensing technologies and Zinc Oxide itself is provided, followed by a study of the potential applications of Zinc Oxide. Later on, the experimental procedure is described, after which the final characterization and results are discussed.

The thesis then concludes that the CBD method, used as a benchmark, provided a better uniformity of growth but the hydrothermal synthesis reaction proceeded at the condition set comprising a growth time of 3.5 hours at 120° C produced a much better morphology. In the end the optimized morphology was put to test for UV and Gas sensing. The corresponding I-V characteristic graphs prove that UV light enhances the gas detection properties of ZnO nanorods.

Table of contents

Table of figures

LIST OF TABLES

1. Chapter 1: Introduction

1.1. Gas sensing technologies

Sensors and transducers have been an important research area since the boom in commercialization of microelectronics. The development of new sensing technologies has enhanced productivity and safety in daily life industrial and domestic activities. Within the vast research puddle of sensors, gas sensors have been under the limelight for quite some time now, not only because of the numerous potential applications they have but also because of the space and requirement for continuous advancements in this specific research field. A number of working principles have been explored and utilized in order to create sensors that are both efficient and durable. Some of the recent technologies utilized include:

Micrmcalorimatric sensor

These consist of an active metal surface continuously maintained at a high temperature (550 ± 50° C) via electric heating. Whenever the sensor is exposed to a certain gas, it burns on the surface in the presence of air. The release of heat increases the temperature of the surface for a short instance, during which the microcontroller reduces the electrical power accordingly to maintain the constant temperature. This reduction in power is characteristic to every gas and is therefore used to detect the presence of various flammable gases.
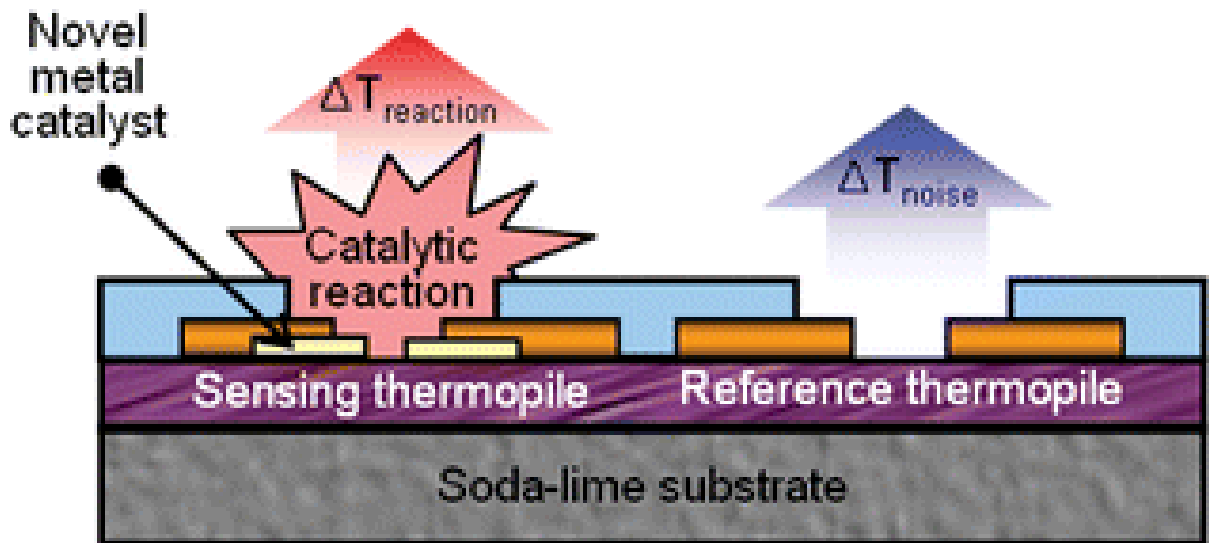
Figure 1 Schematic of a microcalorimetric gas sensor

Electrochemical sensors

These sensors utilize the reduction or oxidation of gas molecules within a circuit M<(variants; two electrode circuit and three electrode circuit) that maintains a fixed circuit voltage at all times. Whenever a gas molecule approaches the transducer's proximity, either an oxidation or a reduction reaction occurs that alters the current. This change of current results in the voltage increasing or decreasing between the electrodes, which is balanced by the rest of the circuit. This change of voltage and the consequent accommodation is characteristic for every gas and is hence utilized as a gas sensing mechanism.
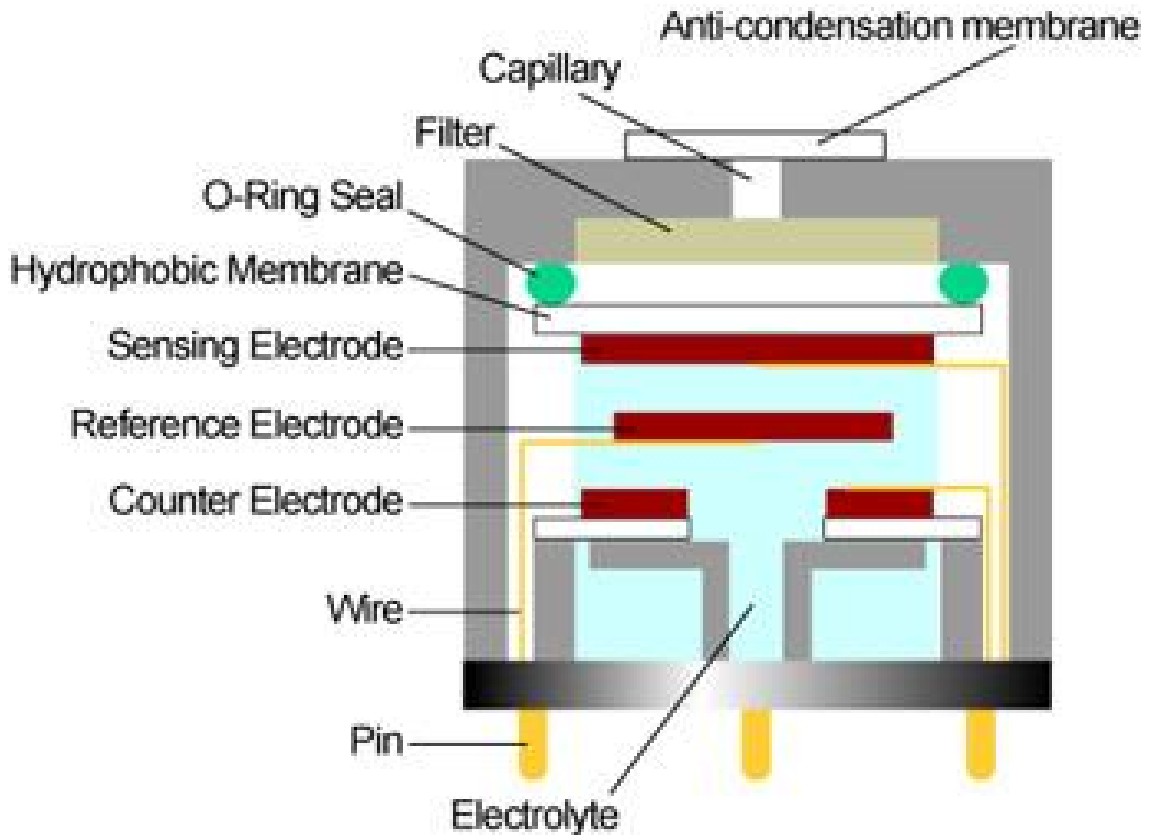
Figure 2Schematic of an electrochemical gas sensor

Mass sensitive/absorption sensors

The mass sensitive sensors utilize rather simple phenomena of change of weight induced by absorption of gas molecules. This change of weight is then leveraged to achieve gas sensing through two principles:

1. Change in resonant frequency due to accumulation of mass
2. Change in refractive index due to accumulation of particles

There are two separate variants of the mass sensitive sensors on the basis of their principle of detection:

1. Resonant frequency based sensors: An absorptive thin film is coated onto a piezoelectric module. The module acts as a resonator and tends to vibrate at a fixed resonant frequency in the absence of gas molecules. Whenever a gas is introduced within the transducer's proximity, the active absorptive film interacts with the molecules. This interaction results in a change of mass of the entire resonator assembly, which results in an alteration of the frequency of resonance. Therefore this shift of frequency is leveraged in order to sense the gas absorbed onto its surface. As the effective absorbing surface area is fixed, the resonant frequency shift will tend to be characteristic for specific gas molecules.

2. Optical refraction based sensors

The absorptive thin film is coated onto a glass substrate and light is passed through it continuously. Whenever a gas passes through the sensor's proximity, it absorbs onto the surface. This results in a change of thickness of the thin layer over the glass substrate, resulting in an alteration in the refractive index of the absorptive layer. This induces refraction in the incident light, which is measured and utilized in sensing.
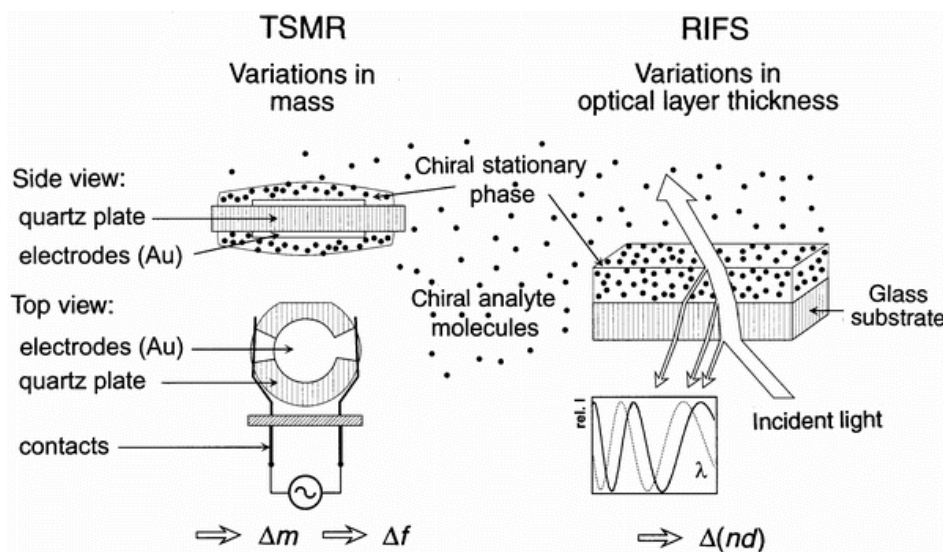
Figure 3; right,Schematic of a microresonator based sensor | Left: Schematic of an optical refraction based sensor

FET Gas sensor

These sensors utilize specialized field effect transistors to sense the presence of Hydrogen gas itself as well as gases that have Hydrogen as a constituent element. The sensing face of the FETs are specially designed to selectively diffuse Hydrogen cations. Whenever a detectable gas approaches the sensing face, it dissociates, which results in the separation of Hydrogen cations. These cations diffuse into the surface and induce a current. The current induction is characteristic to specific gases and their amounts.
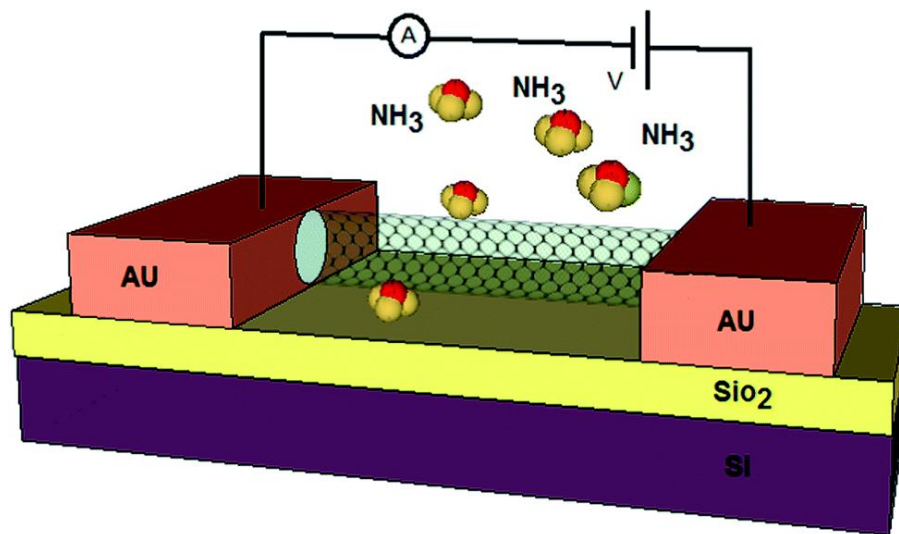
Figure 4 FET Gas Sensor

Metal oxide sensors

In metal oxide gas sensors, an n-type semiconducting metal oxide is deposited on the module. During the absence of a detectable gas, the oxygen from air is trapped onto the metal oxide surface. This entrapment causes the majority charge carriers are attracted towards the adsorbed Oxygen, causing localized potential barrier formation. Whenever a gas that can be oxidized, comes in proximity to the sensor surface, it reacts with the surface Oxygen and releases these electrons, which change the conductivity of the sensing film in that instance. The number of adsorbed Oxygen molecules that react with the incident gas is specific for every gas, and therefore as a result the release of electrons becomes unique for each separate gas. Through the use of this principle, n-type semi-conducting metal oxides can be used as sensors for reducing gases.[6]

Figure 5: left , absence of reducing gas,and right, presence of reducing gas

Image source   : http://www.figaro.co.jp/en/technicalinfo/principle/mos-type.html

1.2. Zinc Oxide

Zinc oxide is a unique, multifunctional inorganic compound that has an appreciably vast range of potential applications. From the research point of view, there are a multitude of reasons that have put Zinc Oxide on the front row for trending research topics since long:

1-Unique properties:

ZnO has been observed to have high chemical and thermal stability at room temperature. Moreover being a direct band-gap semiconductor, it has a wide band gap of around 3.37 eV, which further drops to around 3.44 eV at lower temperatures. It also has a free exciton binding energy of 60 meV, which is considerably a large value in comparison to Ga. ZnO is intrinsically an n-type semiconductor, which is quiet interestingly an anomaly in the general trend of II-V semiconductors. Amongst other properties is the ability of ZnO to absorb a broad range of radiations and has a strong luminescence in the green-white region of the visible light spectrum. ZnO has also been known to have both piezoelectric as well as pyroelectric properties.

2-Convenience of synthesis:

Zinc Oxide is naturally formed due to the oxidation or corrosion of Zinc metal. It is also found in the form of ores. There are multiple methods for the synthesis of Zinc Oxide, some of which include:

-Mechanochemical processes   -Sol gel methods

-Precipitation processes   -Solvothermal techniques

-Hydrothermal techniques   -Emulsion techniques

-Microwave techniques   -Microemulsion techniques

3-Variety of nanostructures:

ZnO boats a wide variety of nanostructures, and almost all of the possible discovered nanostructures can be achieved by tweaking the ZnO synthesis methods. Some of the nanostructures that can be synthesized include, but are not limited to:

-Nanoparticles   -Nanowires
-Nanoclusters   -Nanodisks
-Nanorods   -Nanotubes

4-Potential applications:

Due to its ease of synthesis and a plethora of unique properties, Zinc Oxide is readily used in, and is under research for unveiling its potential in, the following applications:

-

Photovoltaics   -Solar Cells

-Electronics   -Biomedicine

-Sensors and Transducers

Those listed above are amongst other applications, the worldwide consumption trends of ZnO are as follows:
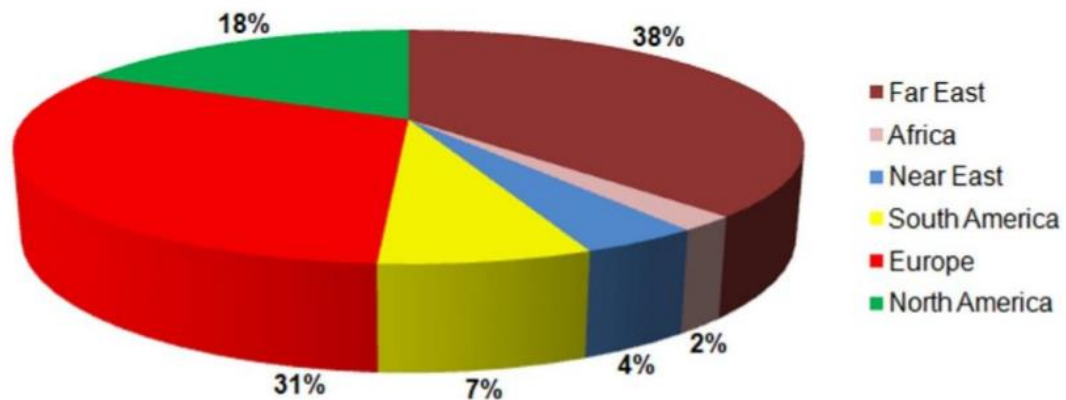
Figure 6 Worldwide consumption of Zinc oxide
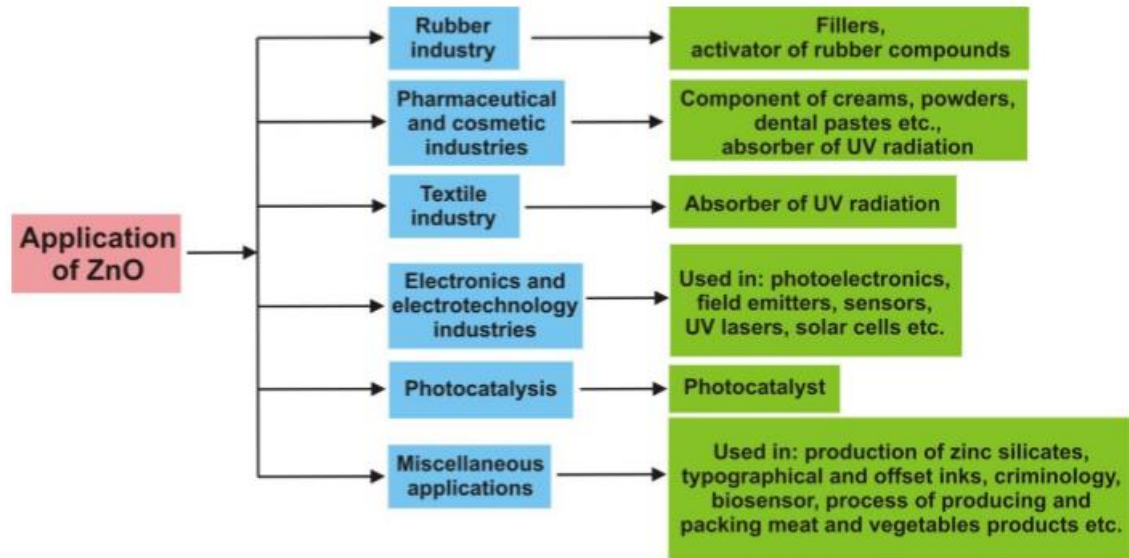
Figure 7 Application routes of Zinc Oxide

5-Lack of health hazards:

ZnO is completely safe to use for humans as well as the environment, and it is therefore the best choice available for products that are eco-friendly and health and safety oriented. Zinc Oxide is inflammable and its constituents, released upon decomposition, are not toxic. Moreover ZnO is also widely accepted to be biocompatible and biodegradable, which makes it suitable for biomedical applications as well.

6-Low cost:

Other metal oxides generally tend to have availability issues as well as a high cost of purchase. Zinc Oxide on the other hand, is both readily available as as well as extremely cost-effective, keeping in mind the fact that it has a huge spectrum of applications[7].

2.Chapter: Literature review

2.1. Basic properties

Table 1:The basic physical properties of Zinc Oxide are tabulated below.[8]

PROPERTIES	
Molecular formula	Zn
Molar mass	81.408 g/mol
Appearance	White solid
Odor	Odorless
Density	5.606 g/cm^3
Melting point	1975 °C (decomposes)
Boiling point	2360 °C
Solubility in water	0.16 mg/100 mL (30 °C)
Band gap	3.3 eV (direct)
Refractive index (nD)	2.0041

2.1.1. Crystal structure

ZnO belongs to II–VI compound semiconductor group whose ionic character is intermediate between that of covalent and ionic semiconductors. It occurs in three crystal structures namely Wurtzite (B4), Zinc Blende (B3) and Rock Salt (or Rochelle salt) of which the Wurtzite structure is thermodynamically stable phase at ambient conditions while the other two can be stabilized and are less common or metastable structures.[9] The three Structures are shown in figures below.

2.1.2. Wurtzite structure

At ambient temperature and pressure ZnO crystallizes as Wurtzite structure. It has a hexagonal unit cell with two lattice parameters "a" and "c" with c/a ratio of 1.633 in an ideal Wurtzite Structure.[9] The Wurtzite structure is composed of two interconnecting hexagonal closed packed (hcp) sub-lattices, in which each sub-lattice consists of Zn or O ions displaced with respect to each other along the threefold c-axis.[4] The Zn ions are surrounded by a tetrahedral of O ions and vice-versa. This polarity is because of the tetrahedral coordination or sp^3 covalent bonding and determines many properties of ZnO like piezoelectricity and polarization. It also plays an important role in the defect generation, crystal growth and etching.[3]

In an ideal case the atoms in each type of sub-lattice are displaced with respect to each other by an amount u= 0.375 in fractional coordinates. .The internal

parameter "u" is defined as the length of the bond parallel to the c-axis (anion–cation bond length or the nearest-neighbor distance) divided by the c lattice parameter. But in real case the Wurtzite structure deviates from the ideal arrangement by changing c/a ratio or "u" value since the experimentally determined value is lower than theoretical.[9]
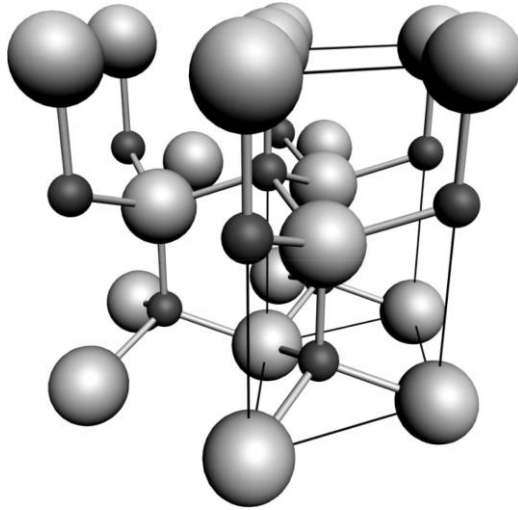
Figure 8 A unit cell of the hexagonal wurtzite structure of ZnO. Large white spheres are O atoms and smaller black spheres are Zn atoms. [3]

2.1.3. Zinc Blende structure

It is a metastable state which can be stabilized by growth on cubic substrates such as ZnS. It is composed of two interpenetrating face-centered cubic (fcc) sub-lattices. These are shifted along the body diagonal by one-quarter of the length of the body diagonal. Each Zinc blende unit cell has four atoms and every atom of group II is tetrahedrally coordinated with four atoms of group VI, and vice versa.[9]

2.1.4. Rocksalt structure

The Rock salt structure cannot be stabilized by epitaxial growth. However, the Wurtzite ZnO to Rock salt transformation occurs at external pressures as high as 10 Gpa and a decrease in the volume of about 17%. As the volume decreases, the inter-ionic coulomb interaction becomes more of ionic nature than covalent.[9]
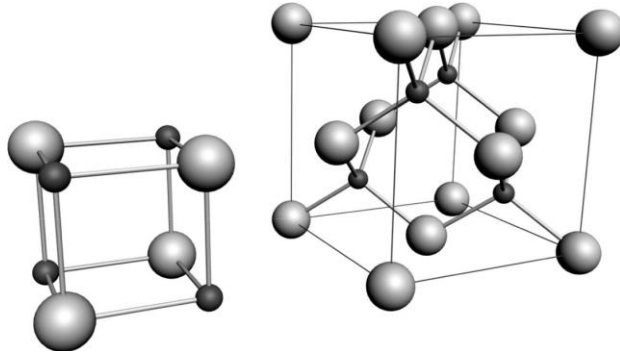
Figure 9 A unit cell of rock salt (left) and zincblende (right) phases of ZnO. White spheres are O atoms, black spheres are Zn atoms.[3]

2.2. Mechanical properties

ZnO is relatively a soft material as the c-axis oriented bulk ZnO has a hardness of ~5 GPa at a penetration depth of 300 nm. The deformation in this material occurs due to slip on the pyramidal and basal planes. Upon contact the defect propagation is larger than the volume under contact. Experiments show that a-axis oriented bulk ZnO has a hardness of ~2GPa at a penetration depth of 50 nm which is lower than c-axis material indicating that the former material is softer. This is because the basal planes are perpendicular to the surface which makes them more susceptible to slip. It strongly indicates that the crystal orientation is detrimental to the mechanical properties of bulk ZnO.[3]

Studies have also shown that the mechanical properties of epitaxial ZnO are different from bulk. For c-axis epitaxial layers, the hardness of ZnO grown on sapphire is ~5.7 GPa.[3]Device applications requiring large electromechanical coupling can use ZnO because its piezoelectric tensor is equal to or even larger than AlN and GaN.[4] The table below exhibits the mechanical parameters of ZnO.[3]

2.3.Properties and device applications

Properties of ZnO that render it useful for device applications are discussed in detail below.

2.3.1. Band gap

ZnO has a wide and direct band gap with values different at different temperatures. As mentioned in[10] the band gap of ZnO is 3.37eV at room temperature and 3.44eV at low temperatures due to which it finds applications in optoelectronics in the blue/UV region, photodetectors, laser diodes and light-

emitting diodes. Reports have also shown that ZnO platelets, thin films, ZnO nanocrystals and ZnO nanowires can be used for optically pumped lasing.

2.3.2. Binding energy

As compared to GaN which has a free-exciton binding energy of 25 meV, ZnO has very large free-exciton binding energy of 60 meV with efficient excitonic emission persisting at room and higher temperatures. Due to these excitonic effects, ZnO is a promising candidate for optical devices.[10]

2.3.3. Luminescence

ZnO is a suitable material for phosphor applications since, it has a strong luminescence in the green-white region of the spectrum with peak in emission spectrum at 495 nm and a very broad half-width of 0.4eV. It can offer services in field emission displays and vacuum fluorescent displays by virtue of its n-type conductivity. The cause of green luminescence has not been confirmed but the acceptor Zn vacancies are more likely to form n-type ZnO.[10]
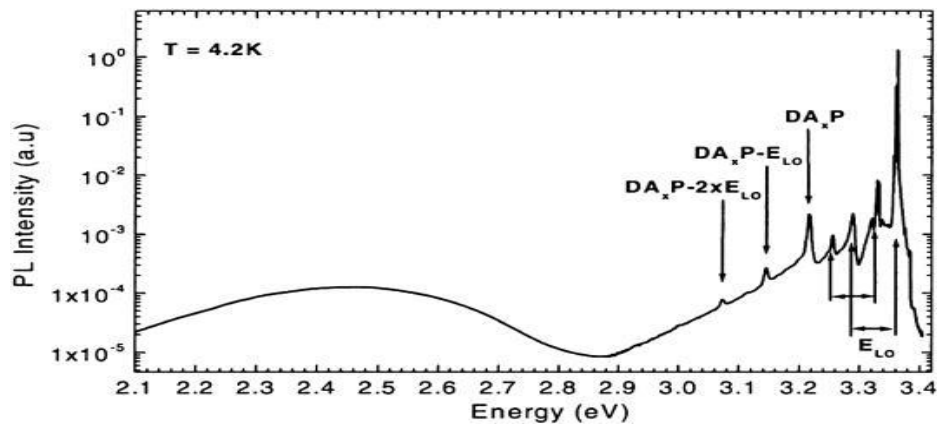
Figure 10 Photoluminescence spectrum of n-type bulk ZnO (HeCd excitation) showing excitonic, donor acceptor pair and green-band emission. The longitudinal optical phonons with the corresponding phonon replicas are indicated on the figure.[3]

2.3.4. Sensitivity and surface conductivity

Zno can be used a sensor to smell the odor. The surface of ZnO thin films is sensitive when exposed to various gases. This attribute can be made useful for detecting the freshness of food and fruits as it are highly sensitive to the presence of trimethylamine in the odor. The mechanism which governs the sensor is not yet clearly defined. Hence, the existence of an electron layer on the surface in vacuum annealed single crystals which disappears upon exposure to air may have encouraged the sensor to act. [10]

2.3.5. Non-linear resistance of polycrystalline ZnO

The semiconducting polycrystalline films with highly non-ohmic current–voltage characteristics are utilized in commercial ZnO varisters. The causes for the non-linear resistance have not been completely understood and many assumptions are made. Yet, the topic is still under consideration.[10]

2.3.6. Optical coefficents

ZnO is appropriate for non-linear optical devices for the thin films show second and thirdorder non-linear optical behavior. The linearity of optical properties of ZnO depends on the crystallinity of the samples. The linearity also depends on the process of growth. For instance, the ZnO films grown by spray pyrolysis, laser deposition and reactive sputtering shows strong second-order non-linear response. Recently, nanocrystalline films have shown third order non-linear response which can be used for integrated non-linear optical devices. [10]

2.3.7. Thermal conductivity

The thermal conductivity, κ (W cm−1 K −1) is a kinetic property determined by the rotational, vibrational and electronic movement. Its importance in semiconductors increases when considering high temperature devices. ZnO contains large number of point defects which influence its thermal conductivity. The thermal conductivity measured from the polar faces of ZnO grown by vapor-phase method is very high as given in [3], which makes its use as an additive in the rubber to increase the thermal conductivity of the tires. High thermal conductivity implies that the rate of heat removal is also high during device operation.[10]

2.3.8. Availability of large crystals

One of the most effective and appealing attribute of ZnO is the availability of large single crystals. Crystals can be obtained by techniques such as hydrothermal growth, vapor-phase transport etc. Thin films can also be obtained by chemical vapor deposition, sputtering and ultrasonic spray chemical vapor deposition. The formation of ZnO thin films on substrates is of great potential as compared with GaN since ZnO has reduced concentrations of defects and it could even surpass the efficiencies obtained by GaN.[10]

2.3.9. Radiation hazards

ZnO exhibits very high radiation hardness even greater than GaN which makes it useful for applications at high altitudes or in space, due to the importance of radiation hardness in these regions.[10]

2.3.10. Amenability to wet chemical etching

The amenability of ZnO thin films to be etched by various mixtures including acids and bases at low temperatures makes it flexible in processing, designing and integration of devices.[10]

2.4. Nanostructure of Zinc Oxide

Nanostructures can be classified into four basic categories [11]

i-0D Nanostructures: Nanoclusters, Nanoparticles and Nanodots/Quantumdots

ii-1D Nanostructures: Nanorods, Nanotubes and Nanowires

iii-2D Nanostructures: Nanoplates, Nanodisks and layers iv-3D Nanostructures Nanotetrapods, nanoflowers etc

2.4.1. Nanoparticles

part of Nanomaterials having diameter in the range of 1-100 nm. Nanoparticles exhibit important electrical, optical and magnetic properties and can be used in applications such as sensing, optics, energy storage, environment protection and medicine. Different types of nanoparticles are discussed in the literature like metal oxide nanoparticles, polymer nanoparticles, and metal nanoparticles. The most versatile among them are metal oxide nanoparticles due to their properties and functionalities. Among different materials, ZnO nanoparticles are of great importance. They are used as gas sensors, solar cells, chemical sensors, optical and electrical devices, bio-sensors etc.[4]

Various routes have been adopted to fabricate nanoparticles. Hence, the sol-gel method is cheap, easy to handle, reliable, repeatable and environment friendly. ZnO nanoparticles were synthesized using various routes. The sol–gel method proved a successful synthetic route in terms of its cost, ease of handling, reliability, repeatability, and environmental friendliness.ZnO nanoparticles act as an effective UV-blocking material as compared to TiO2 and can be used in cosmetics for protection of skin.[4]

2.4.2. Nanorods

These are cylindrical structures having a high aspect ratio (length to diameter) but the aspect ratio is less than that of nanowires. The growth direction is usually along the c-axis and the crystal structure is hexagonal Wurtzite.
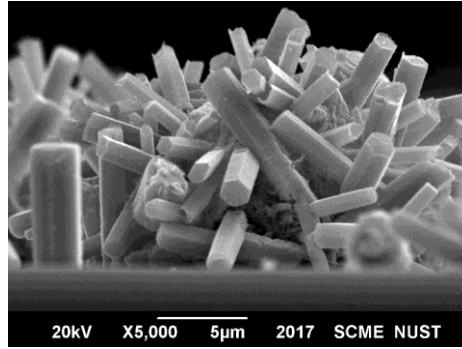
Figure 11 SEM image of Nanorods grown on ITO glass substrate by hydrothermal method.

2.4.3. Nanowires

Nanostructures having a high aspect ratio are called nanowires. The lengths are in tens of microns and the crosssectional diameters are << 1um as defined in [12]. They can be synthesized by various methods including vapor phase methods, thermal oxidation, hydrothermal growth, metalorganic chemical vapor deposition etc.[13] Nanowires can be used for applications such as solar cells and gas sensors.
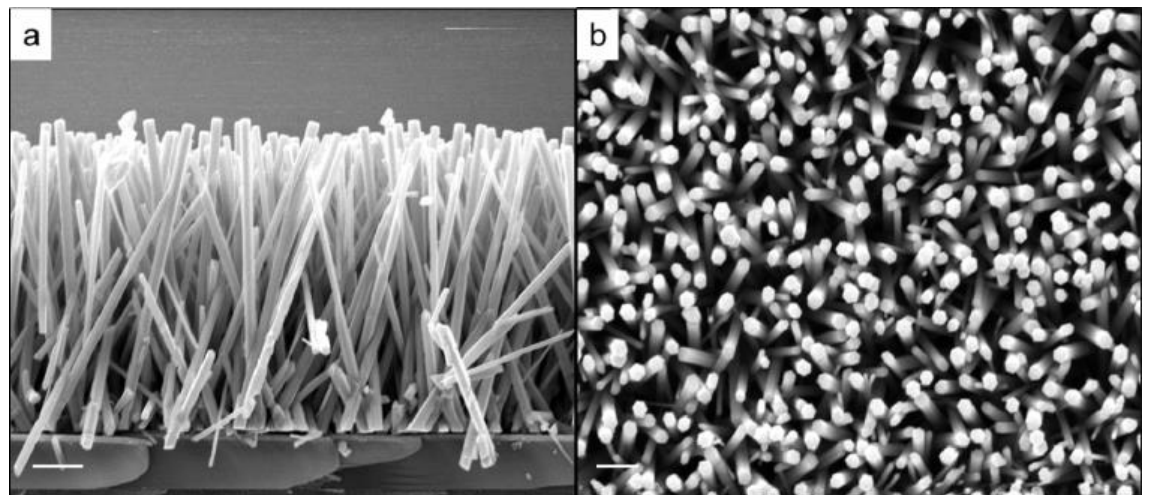
Figure 12 SEM images of nanowires, (a) edge view, (b) top view

2.4.4. Nanotubes

The hollow, tubular nanostructures with increased surface area and porosity than that of Nanorods and nanowires are nanotubes and, thus, have greater potential

for enhanced performance and activity, such as adsoption, entramolecular junctions, catalysis, and biosensors. Figure 8. TEM images of the as-synthesized ZnO nanobelts.[2]

Although, the growth methods for ZnO nanotubes have not been studied in depth. However, few methods such as hydrothermal decomposition, thermal oxidation and evaporation, and plasma-assisted growth are commonly used.[14]
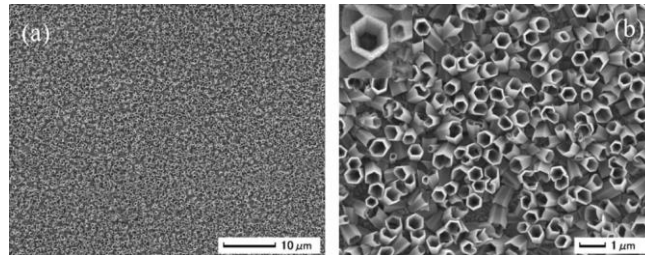
Figure 13 SEM image of ZnO nanotubes.[1]

2.4.5. Nanobelts

Nanowires with a well-defined geometrical shape and side surfaces are called nanobelts. The synthesis of Nanobelts of ZnO occurs by sublimation of ZnO powder without a catalyst. The typical thicknesses and widths of nanobelts are in the range of 10-30 nm and 50-300 nm respectively. The cross section is rectangular, width is uniform along the length, and the width-to-thickness ratio is~5 to 10.[2]
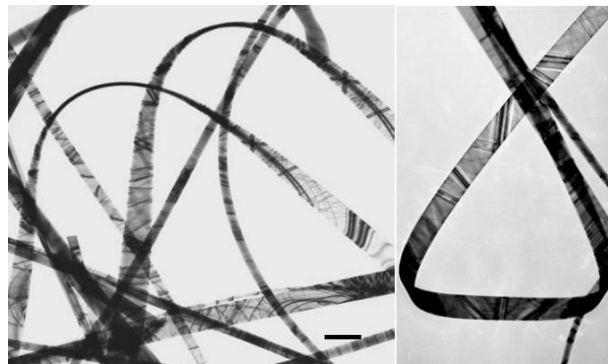
Figure 14 TEM images of the as-synthesized[2]

2.4.6. Hierarchical nanostructures

If the composition of the source material is changed, the morphology of the nanostructures can be changed and complex, hierarchical nanostructures can be obtained. For instance when ZnO and SnO2 are mixed in a 1:1 weight ratio, Sets of central axial nanowires, surrounded by radically distributed nanobranches are formed. The formation of these structures is governed by

VLS growth mechanism. The growth proceeds in two stages. During the faster first stage, nanowire growth occurs. The second slower step results in the nucleation and epitaxial growth of nanoribbons on the six crystallographic directions of the nanowires spaced at 60∘ to each other.[2]

Figure 15 SEM image of the hierarchical ZnO nanostructures.[2]

2.4.7. Nanocombs and nanosaws

Since the anisotropic growth is a common characteristic of the wurtzite family, the comb structure is the result of an asymmetric growth occurring along Zn [0001]. This is because Zn has two surfaces. The positively charged Zn (0001)surface is chemically active and the negatively charged O-(000$\bar{1}$) surface is relatively inert. Experimental results indicate that the chemically inactive (000$\bar{}$ 1) surface typically does not grow nanobelt structure. Hence, the Zn-terminated (0001) surface has tiny Zn clusters, which could lead to self-catalyzed growth without the presence of foreign catalyst.[2]

Figure 16 SEM image of nanocombs and saws.[2]

2.4.8. Nanosprings and nanospirals

A spiral shape is formed when a polar nanobelt reduces its electrostatic energy by rolling over into an enclosed ring. Similarly the formation of nanosprings and nanohelixes is an effort of the polarized surface to minimize or neutralize the dipole moment, lowering the electrostatic energy. Each nanospring is made of

uniformly deformed single crystal ZnO nanobelt. It has a radious of~500-800 nm and a uniform shape with evenly distributed pitches.[2]

2.5.Potential applications of Zinc Oxides

2.5.1. Domestic

Currently, ZnO is used in health care products to protect the skin from sun damage, help slow down progression of age-related degeneration, and provide mineral in food additives.

2.5.2. Industry

Nano-scale ZnO is utilized in rubber industry for efficient production of anti-abrasion rubber. It is also important material in ceramics industry since it serves as white dyestuff to lower sintering temperature. Chemical industry uses ZnO for producing deodorant and antibacterial materials. Last but not least, the paint industry is benefitting from ZnO by improving shielding and anti-static materials.[5]

2.5.3. ZnO nanowires solar cell

Highly efficient nanowire solar cells can be fabricated by using ZnO NWs as charge collectors and n-type semiconductor. The efficiency of solar cells using the nanowire geometry is enhanced as compared to simple thin films due to improved charge collection and separation, reduced reflection and light trapping capability. The energy conversion efficiency is also increased due to increased p-n junction area in the NW structures leading to increased short cicuit current.When the photovoltaic effects of Cu_2O/ZnO NW cells were measured with illumination through the ITO glass substrate and the results were compared with Cu_2O/ZnO planar thin film junctions, it was found that the short circuit current density of the NW junctions is 8.2 mA/cm2 , which almost doubles that obtained from the planar junctions (4.3 mA/cm2).[5]
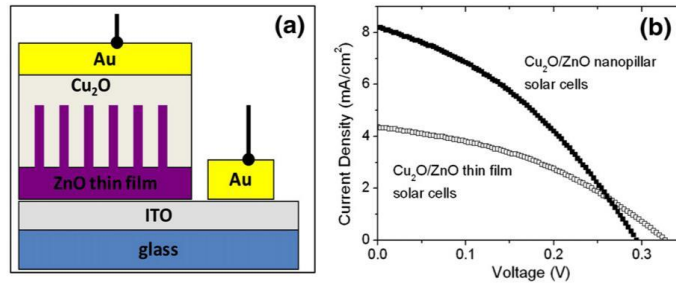
Figure 17 (a) Device structure of ZnO NWs solar cell (b) current density versus voltage graph of ZnO/Cu2O NW solar cells.[5]

2.5.4. Photo detectors

Nowadays, photodetectors with UV spectral response have huge potential applications in spectroscopy and sensing requiring the detection of UV light without the influence of visible or infrared light to minimize the background signal and avoid erroneous detection. ZnO NWs can be used for fabricating photodetector arrays due to their peculiar material properties such as single crystalline structure of individual NWs. Advantages of using ZnO NW photodetectors are: i) wide bandgap (3.3 eV) with no response to visible and infrared light; ii) Large exciton binding energy allowing it to work at elevated temperatures; (iii) high saturation velocity for potentially high operation speed; (iv) exceptionally resistant to radiation damage; and (v) since each NW can be used as a detection element, it is capable of achieving higher spatial resolution as compared to thin film structures.[5]

2.5.5. ZnO thin films as methane sensors

Literature shows the sensitivity of ZnO thin films to Methane (CH4). In an experiment the sensor element comprised of a chemically fabricated ZnO semiconducting layer and a layer of palladium (Pd) as catalyst. A reasonable sensitivity of approximately 86%, fast response time of less than one minute, and a moderately fast recovery (approximately 3 minutes) was observed at 200oC.[15]

2.5.6. Nanocantileves

The cantilever based scanning probe microscopy (SPM) technique is one of the most powerful approaches in imaging, manipulating and measuring nano-scale properties and phenomena. The conventional cantilever used for SPM is based on silicon, Si3N4 or SiC. Utilization of nanowire and nanotube based cantilevers can have several advantages for SPM. Carbon nanotubes can be grown on the tip

of a conventional cantilever and used for imaging surfaces with a large degree of abrupt variation in the surface morphology.

Combining micro-electromechanical system (MEMS) technology with self-assembled nanobelts has produced cost effective cantilevers with much higher sensitivity for a range of devices and applications. Semiconducting nanobelts are suitable for cantilever applications beacuase they are defect free single crystals with excellent mechanical properties.Additionally, the cantilever sensitivity is increased by reduction in dimensions of nanobelt cantilevers. Combining the aforementioned techniques with micromanipulation has led to the horizontal alignment of individual ZnO nanobelts onto silicon chips.The resonance frequency of each cantilever can be tuned and they can be modified for different applications such as contact, non-contact and tapping mode AFM. [2]
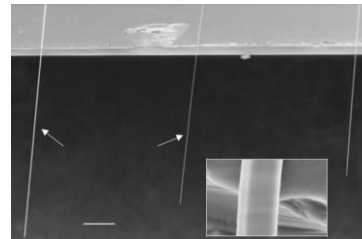
Figure 18 highly aligned nanobelts as nanocantilever arrays on silicon chip.[2]

2.6.Synthesis methods for ZnO nanostructures

The synthesis methods of ZnO nanostructures can be classified into following two broad categories. Solution Phase Synthesis: As the name implies, the process is carried out in liquids mainly aqueous solutions. Some largely utilized solution phase synthesis methods are as follows:

1. Sol-gel Route   3. Electrophoresis

2. Spray pyrolysis method   4. Hydrothermal

2.6.1. Sol-gel method

Zinc Oxide nanostructure can also be synthesized by using sol-gel method. First, a sol is prepared. For this, 2 g of Zinc Acetate Dihydrate and 8 g of Sodium Hydroxide are weighed using a weighing balance. Then, 10 ml and 15 ml of distilled water are measured by a measuring cylinder and placed separately. Then, 8 g of sodium hydroxide is dissolved in a 10 ml of distilled water and 2 g of Zinc Acetate Dihydrate is dissolved with a 15 ml of distilled water. Both the

19

solutions are stirred for about five minutes each. After a fine mixture is achieved, the sodium hydroxide solution is poured to the solution containing zinc acetate and stirring is continued. Then, 100 ml of ethanol is poured drop wise to the solution containing both sodium hydroxide and zinc acetate. Finally, white precipitate was formed which indicate that the reaction has occurred.[16]

2.6.2. Spray pyrolysis method

This simple and low cost method is used for large area coatings and thin films. One of the major advantage of using this technique is reproducibility, ease of adding materials and mass production capability. Conventional methods include the use of oxygen, nitrogen or air as carrier gases to transport the precursor solution but the new techniques use atomizers for the spray. This prevents the deposition of large droplets and enhances the wettability between particles and the deposited layers.

The solution for the growth of nanostructures is prepared and mixed thoroughly using a magnetic stirrer. The substrate is cleaned using organic solvents like ethanol. It is heated and a constant temperature is monitored using a thermocouple. The precursor solution is atomized and sprayed at a fixed distance from the substrate. The spraying step is done in intervals so the substrate re-attains its temperature. The coated substrates cool to a room temperature. The reaction using a $ZnCl_2$ solution is as under[17]:

$$ZnCl_2 + H_2O \Rightarrow ZnO + 2HCl$$
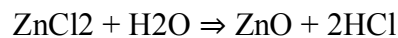
2.6.3. Electrophoresis/ electrophoretic deposition

This technique is used for producing films of nanoparticles. The process is carried out in an electrophoretic cell. The thin films are deposited on the substrate which is the working electrode and the counter electrode is usually platinum foil. These are separated by a specific distance. The EPD is carried out under galvanostatic conditions, predetermined current densities and deposition times. The substrate is allowed to dry at room conditions.[18]

2.6.4. Hydrothermal method

The advantage of using this method is that the reaction at higher than 100 C temperatures can be performed and the process is user friendly and produces highly oriented nanostructures. Certain amounts of Zinc nitrate hexahydrate and

Hexamethylenetetramine (HMTA) are mixed and stirred in a beaker containing distilled water for 30 minutes[19]. After this the mixture is poured inside a Teflon lined autoclave vessel containing the substrate. The vessel is tightly closed and placed in oven for suitable growth time and temperature. After the completion of growth process the substrate is taken out of the vessel and cleaned with distilled water and ethanol.[20] The reactions that occur in the vessel when Hexamethylenetetramine and Zinc nitrate hexahydrate are used a growth solution[21]:

Decomposition reaction: $(CH_2)_6N_4 + 6H_2O \longrightarrow 6HCHO + 4NH_3$

Hydroxyl supply reaction: $NH_3 + H_2O \longleftrightarrow NH_4+ + OH$

Supersaturation reaction: $2OH- + Zn_2+ \longrightarrow Zn(OH)_2$

ZnO growth reaction: $Zn(OH)_2 \longrightarrow ZnO + H_2O$
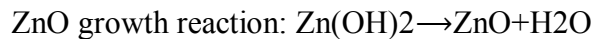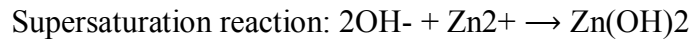
2.6.5. Gas phase synthesis

The growth of nanostructures is carried out in closed chambers at high temperatures using the gaseous environment. Some common methods using gaseous environment are discussed below.

1. Vapor transport method

2. Microwave assisted heating

3. Metal organic chemical vapor deposition

4. Ultrasonic spray chemical vapor deposition

2.6.6. Vapor transport method

This process for the growth of ZnO particles takes place inside the Quartz tube placed in a thermal furnace. The substrate of desired material for example silicon is placed in the center of the Quartz tube at a distance of Zinc source. The growth process takes place in steps. (1) Argon gas flows through the tube for 0.5 hour to remove the air. (2) The furnace temperature is increased to 800°C while the Ar gas is flowing. (3) The temperature of the furnace is kept at 800°C for 1 h and the Argon gas flow is replaced by a mixture of either Ar/H2O vapour or Ar/O2 gas. During the process, the pressure of the quartz tube is kept at 0.03~0.05 MPa. (4) The sample is cooled down to Room Temperature at the rate of 7°C per minute. Following reactions of metallic Zn with H2O vapour and O2 gas occur, respectively.[22]

$$Zn_{(g)} + H_2O_{(g)} \rightarrow ZnO_{(s)} + H_{2(g)} \quad (1)$$
$$2Zn_{(g)} + O_{2(g)} \rightarrow 2ZnO_{(s)} \quad (2)$$
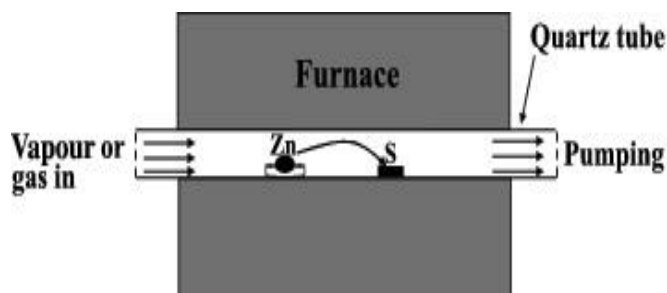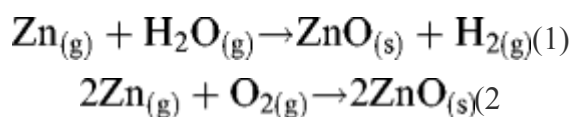
Figure 19 Vapor phase growth of Zn particles on Silicon substrat

2.6.7. Ultrasonic spray chemical vapor deposition

Generally, one-dimensional (1D) ZnO nanostructures are fabricated by the vapor transport method and metal organic chemical vapor deposition (MOCVD). However, the former process is not suitable for fabrication of multilayers or doping, and the latter uses dangerous and expensive materials. To overcome these issues, an ultrasonic spray CVD or mist-CVD method is utilized. This method is an improved and advanced version of the spray CVD or the spray pyrolysis method. Since the spray pyrolysis method is well known fabrication technique for thin films, the USCVD adds an extra benefit of easy doping and safe handling of source materials.[23]

The growth parameters and process is demonstrated. The gold or any other suitable metal catalysts are used for the synthesis of ZnO nanostructures. ZnO nanostructures are expected to grow via a vapor-liquid-solid (VLS) growth mode so Au thin films are deposited by vacuum evaporation on substrates. The Au thin films coagulate to form Au particles when heated at the growth temperatures but before the growth starts. These Au particles serve as catalyst for the VLS growth mode. The solution for the Zinc oxide source is zinc acetate dehydrate (Zn(CH3COO)2H2O) in a mixture of water and acetic acid (90:10). The advancement in this technique is the utilization of aerosol particles atomized by an ultrasonic transducer from the solution as the CVD precursors instead of vaporized sources in conventional MOCVD. The growth temperatures for the synthesis of ZnO nanostructures are $750 - 950$ ∘C. The oxygen gas transfers the aerosol particles to the tube where the substrate is placed and reaction proceeds for 30 minutes.[23]

22

2.6.8. Microwave heating

This method uses a chemical bath with the substrate immersed inside the solution so it is also called chemical bath deposition for the ZnO Nanorods synthesis. First, a precursor solution is prepared by stirring a mixture of zinc nitrate hexahydrate (Zn(NO3)2 6H2O) and hexamethylenetetramine (C6H12N4; HMTA) in de-ionized (DI) water at room temperature for 30 min to obtain a well-dissolved solution. It is then placed into a microwave oven and heated until the solution attains temperature of 95 C with constant magnetic stirring. Once the temperature is achieved, the precursor solution is further heated by the microwave oven at a constant temperature of 95 C with magnetic stirring for 2 h. The following reaction takes place as stated in[24].

$$(CH_2)_6N_4 + 6H_2O \rightarrow 6HCHO + 4NH_3$$

$$NH_3 + H_2O \rightleftarrows NH^+ + OH^-$$

$$2OH^- + Zn^{2+} \rightleftarrows ZnO + H_2O$$
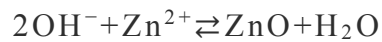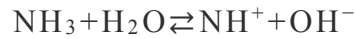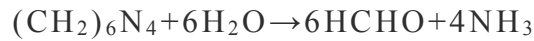
As the reaction proceeds, the solution becomes unclear and translucent. This indicates that the reaction has occurred and the formation of Nanorods is taking place. The Zn2+ ions dissociated from the zinc nitrate react with OHions to form the Nanorods. The solution is left to cool down to room temperature and the substrate is taken out. It is rinsed with distilled water and dried.[24]

3.Chapter 3: Experimental procedure

The project was experimentally divided into two phases:

1-Synthesis Phase

2-Sensing Phase

3.1.Synthesis phase

The synthesis phase involved optimization of the synthesis process of ZnO nanorods in order to achieve:

-Higher uniformity of arrays

-Higher aspect ratio of nanorods

 -Better ment of arrays

-A scalable and reproducible synthesis route

 This phase was further divided into the following steps:

3.1.1. Choice of substrate

After sufficient literature review it was concluded that seeding the substrate at least minimizes, and usually eliminates any effects of substrate's inherent crystal structure on the nanorod morphology.

Choice of substrate was therefore influenced by:

-Availability

-Transparency

-Conductivity

The substrate that was eventually chosen for this project was ITO coated glass.

3.1.2. The choice of synthesis process

The method chosen for synthesis of ZnO nanorods was the hydrothermal method. In general, the hydrothermal method can be defined as:

High temperature and pressure reaction that involves aqueous solutions of the reactants.

This method of synthesis was chosen for the following reasons:

-High temperature growth

-Availability of reactants

-Better control over nanorod morphology

-Customizable, convenient to optimize

The two methods then chosen for benchmarking were CBD and Hydrothermal processes.

3.1.3. Reactants and apparatus
The following reactants were used in each stage:
-**Seeding**:
  -Zinc Acetate
  -Ethanol
-**Growth**:
  -Zinc Nitrate Hexahydrate
-Hexamethylenetetramine (HMT)
-Distilled water
The apparatus utilized throughout the experiment consists of:
-

Petri dishes –	-Electronic weight balance
Beakers	-Muffle furnace
-Drier	-Autoclave furnace
-Foreceps	-Spatula
-Magnetic stirrer	

3.2. Synthesis steps

The synthesis of ZnO nanorods using the Hydrothermal reaction occured in three steps:

-Substrate seeding

-Hydrothermal growth

-Annealing

3.2.1. Substrate seeding

The substrate was seeded via two different methods.

Seeding Solution:

5 mM solution of Zn Acetate in Ethanol was prepared first. Exactly 0.0547 grams of Zn Acetate was mixed in 50 ml of Ethanol and stirred for a few minutes.

Seeding Methods:

Initially the seeding method adopted was the dip-coating method, however the lack of proper uniformity prompted the use of spin-coating method, which gave the required seed layer uniformity (confirmed via pre-growth AFM of seed layer and post-growth uniformity observed in SEM).

Seeding Procedure:

The substrate was first delaminated and cleaned by sonicating them inside an Ethanol bath. For the dip coating method, the substrate slide was then dipped into the seeding solution and quickly drawn out and dried. For spin coating(dynamic), the substrate was placed on the spin coater and a drop of 40 microliters was dropped on the specimen, rotating at 3000 RPM.

3.2.2. Hydrothermal growth

The seeded substrate slide is placed inside a Teflon container filled with 25 mM Zn Nitrate Hexahydrate and 25 mM HMT solution in distilled water.

The container is sealed and placed inside the autoclave. The temperature is set to rise at 10 degrees per minute to a peak value that is variable, discussed under experimental design. The amount of time allowed for the reaction to stay at the peak value of temperature, the growth time, is also an experimental design variable. After the fixed growth time has passed, the heating is turned off and the slide remains inside the autoclave to gradually attain ambient temperature.

3.2.3. Annealing

After the hydrothermal growth process, the sample is placed inside a muffle furnace for annealing. The furnace is set to attain an annealing temperature of 450 degrees (ZnO recrystallization temperature) at a rise rate of 5 degrees per minute. Once the temperature is attained, it sustains for a soaking time of 1 hour. The slide is then left inside the furnace to ensure prolonged, gradual cooling.

3.3. Characterization

The following characteristics of of ZnO nanorods are relevant for the goal of our project:

-Crystallinity   -Uniformity

-Alignment   -Orientation

-Morphology

These characteristics can be studied using the following characterization techniques:

-XRD

-SEM

3.4. Experimental design

In order to achieve high-aspect ratio nanorods, the process parameters must be altered accordingly. Therefore design factors and variables are mapped out first. The variables in this experiment are:

  -Substrate placement

  -Growth time

  -Growth temperature

3.4.1. Substrate placement

During the Hydrothermal growth of ZnO nanorods, sometimes homogeneous nucleation results in precipitation that settles down under the action of gravity. Conventional sample placement techniques can cause collection of precipitates on the growth surface.

The choice of substrate placement was of foremost importance as in the later experimentation, during the detailed/resolved tweaking of parameters, the substrate orientation inside the vessel was to be kept constant.

There were three different substrate placement orientations to choose from:

-Sideways placement

-45 degrees slanted placement

-Inverted substrate mounting

3.4.2. Sideways placement

The sideways placement was inspired from the Chemical Bath Deposition method of ZnO nanorod growth, and could be replicated inside the Teflon vessel using a grooved Teflon stub as a stand.

Benefits

-Substrate surface exposed to a greater volume of reactant solution

 -Relatively easier extraction of substrate from the vessel (arrangement dependent)

3.4.3. Slanted placement

The 45 degrees slanted placement allowed an inverted, but tilted substrate.

Benefits:

-Relatively easier placement

-Doesn't allow precipitation (caused by homogeneous nucleation) to settle on the growth surface

3.4.4. Inverted placement

The inverted sample placement was achieved using a lid, specifically designed for this project, in order to mount/hold the substrate in an inverted position as the reaction occurred.

Potential Benefits:

-Easiest placement and extraction of substrate

-Exposure of substrate surface to a sufficient volume of reactant solution (greater than 45 degrees slanted position)

-Fixed area of growth with margins

-Highly reproducible and scalable

-Elimination of the probability of precipitate settlement on growth surface

3.5. CAD and manufacturing accessories

We designed, and had the accessories manufactured at the Manufacturing Resource Centre, SMME ourselves for the required reaction alterations. These include:

3.5.1. Design of inverted lid mounting

For the inverted placement of the substrate, a lid mounting assembly had been designed. The assembly consists of a separate lid for the Teflon vessel that allows inserting the substrate inside. Once inserted, the slide's growth surface faces downwards into the vessel, where a sufficient volume of reactant solution is available to interact with it. The exposing window's design allows capillary action to ensure the reactant solution stays in contact with the substrate surface throughout the reaction. Upon completion of the reaction, the lid can easily be lifted, bringing the substrate out of the vessel along with it. The substrate can then be slid out for further procedures.
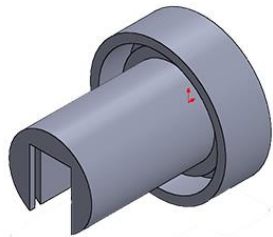
Isometric view

Setbacks and re-designing:

The inverted lid design's first iteration failed to keep the samples intact, and the alignment issues along with the pressure exerted on the slide by the fluid's surface tension resulted in cracking or damaging of the ITO slides. Consequently, the inverted placement add-on for the vessel had to be redesigned and the "sleeve" design was conceived:

The sleeve design allowed:

  -Secure and locked placement of sample without fluid pressure or alignment issues

-Locking of the sample to keep it fixed

-Easy fluid removal and washing of the sample

-Minor cutting of sample as compared to previous design

3.6. Determination of best substrate orientation

In order to decide which substrate placement orientation should be adopted, a series of experiments had been designed in order to measure the effect of each substrate placement on surface morphology, under similar time and temperature conditions. The series of experiments that were conducted is as follows:

Table 2: Condition set matrix

	Growth Temperature		
Growth Time	100° C	120° C	140° C
2hr 30m	-Slanted -Vertical -Inverted		
3hr 30m		-Slanted -Vertical -Inverted	
4hr 30m			-Slanted - Vertical -Inverted

SEM images were utilized later on in order to conclude which of these condition sets worked best for achieving the required morphology.

3.7. Choice of growth condition

The growth conditions consisted of two variables:

-Growth time

-Growth temperature

The range for growth time was kept between 2.5 hours to 5.5 hours with the increment of 1 hour. The range for growth temperatures was from 100° C to 160° C with an increment of 20° C. The discrete conditions are listed in the matrix above.

Later on in the experimentation phase, the extreme highest condition set, growth at 160° C for 5.5 hours was excluded from the experimentation due to certain limitations and the above matrix was reduced to a total of only nine experiments.

Benchmarking:

In order to have a reference for proof of optimization, we used the synthesis procedure currently in use by Miss Shazrah Shahzad in her masters research work. The benchmarking synthesis method involved growth using CBD at the following parameters:

Growth temperature: 90° C

Growth time: 2.5 hours

3.8. Sensing phase

In the sensing phase, the following major steps were followed:

1-Sensor Design

2-Sensing Chamber Design

3-Assembly

3.8.1.   Sensor design

The sensor was designed by making connections at two different regions on the slide: 1-Exposed ITO

2-Nanorod growth area

In order to achieve the exposed ITO, the samples were masked during seeding via masking tape and later on covered by using the autoclave tape in order to keep a certain area from involving in any reactions and hence achieved an exposed ITO surface.

The connections were then made as the following illustration shows:

Copper contact with ITO

ZnO nanorod on ITO

Copper contact with ZnO nanorods
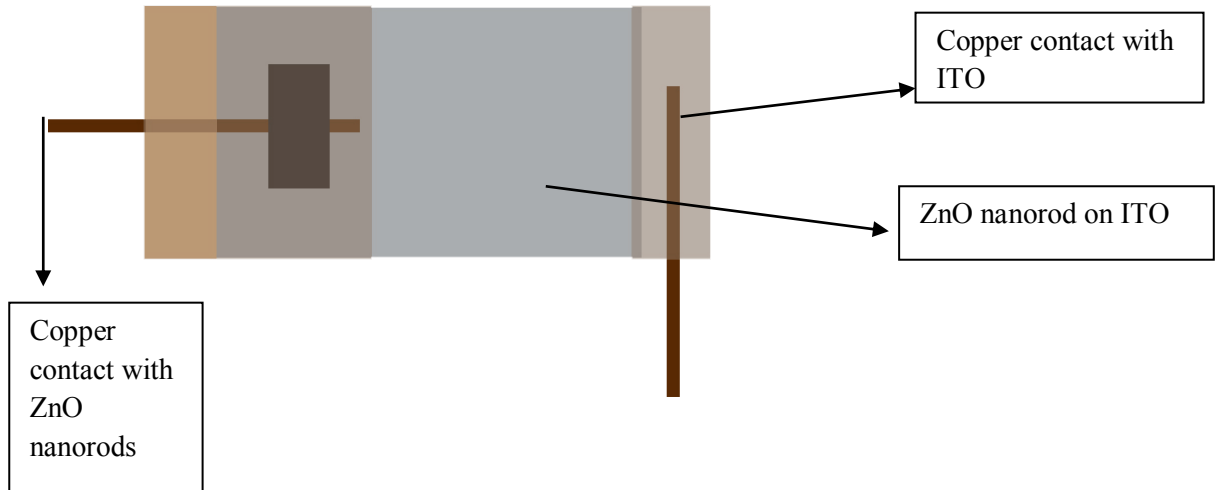
3.8.2. Chamber design

A specialized sensing chamber, consisting of a fixed volume and contained conducting clamp connections was sealed after being installed with a UV lamp inside it. The initial structure of the chamber was designed and manufactured by Mr Muzzamil Ahmad, a Masters student at SCME.

3.8.3. Assembly

The sensor was placed inside the chamber and it was sealed. Afterwards, the chamber was connected to a flow-meter that mixed and measured flows of gases coming from two separate containers.

The connections made with the clamps to which the sample was attached, were connected with the Biologic VSP apparatus for the I-V Characteristic measurement.

Carrier gas (N₂)

Sensing chamber

Display

Methane gas

Mixer

Electrical station

32
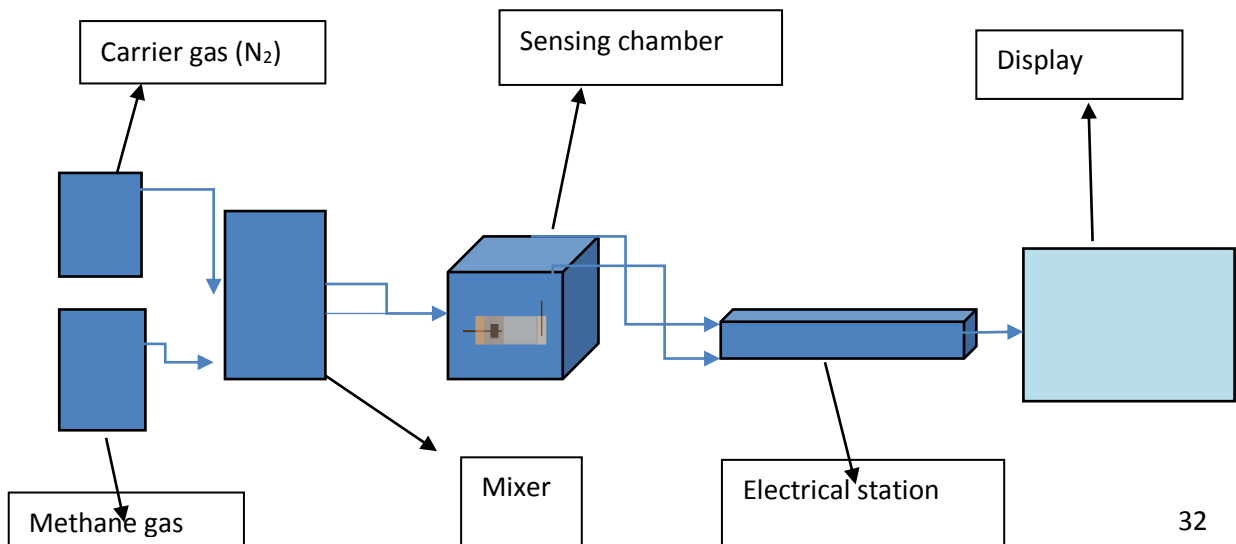
4. Chapter 4: Characterization, results and analysis

The following characterization techniques were used to find different properties and results

1. Scanning Electron Microscopy (SEM)

2. X-Ray Diffraction (XRD)

3. IV characteristics

4.1. Scanning electron microscopy

SEM is the powerful technique to characterize various kinds of materials. One can find its frequent use in metallurgy, biology, medicine, geology etc. The basic purpose of SEM is to study the morphology topography, chemical composition, crystal structure and electrical behavior of very small samples[25].

There are two main components of SEM which are electron console, electron column, vacuum system, display and electronic controls. The basic function of the electron console is to control the switches and knobs which actually help in the adjustment of instrument which includes accelerating voltage, filament current, magnification, contrast, brightness and focus

4.1.1. Image formation in SEM

The SEM images are quite different from the images taken by light microscope[25]. The electron column contains 2 or more electromagnetic lenses which are operated in vacuum and electron gun. The electron gun accelerates the electrons giving the high energies in the range of 1-40KV[25]. The electron laser is used to create focused probe on the samples[26]. Probe diameter can define the electron beam i.e. in the range of 1 nanometer to 1 micrometer. Probe current ranges from pA to μA; and probe convergence ranges from 10-4 to 10-2 radians. To take the image the electron beam is focused into the fine probe, then the surface is scanned using scanning coils figure. 22

Scannning Electron
Microscope (SEM)

Electron Gun

Anode
(accelerator)

Electron beam

Magnetic
lenses

Detector

Sample
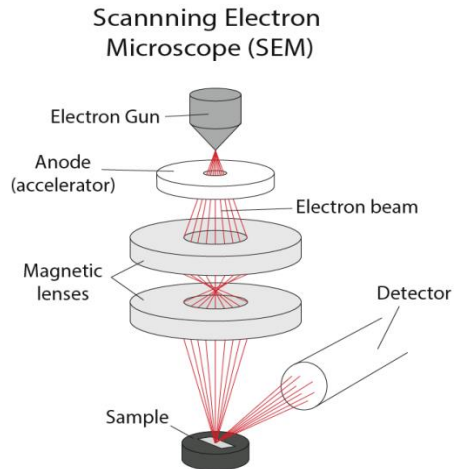
Figure 20 schematics of SEM

Signals in the form of electromagnetic radiations are generated when the each of the part of the specimen is struck to the high speed electrons. Out of these radiations, back scattered electrons are secondary electrons are collected by the detector and then the signal is amplified and the image is displayed on the monitor screen. This image is easy to interpret. The ointeraction depth is about 1 micrometer. Usually the quality of the SEM images depends on three important parameters.

1. Performance of the instrument

2. Imaging parameters

3. Nature of the specimen

4.1.2. Lenses

The function of lens is to converge the electron beam, so that a beam of desired diameter is produced. They are cylinders of metal operating in vacuum. Magnetic field is generated inside the lens to focus of defocus the electron beam.

Lenses have three basic designs

1. Conical lens or Pinhole :- specimen is outside the lenses and magnetic field

2. Immersion lens:- for very small specimens which are to be placed inside the lens

3. Snorkel lens:- specimen is inside the magnetic field, but outside the lens.

4.1.3. Magnification in SEM

The magnification of SEM is defined as the ration of the scan line length on the monitor to the scan line length of the specimen that is why it is independent of the lens. Mostly, the display or screen length is fixed; the only way to change the magnification is by increasing or decreasing the scan length of the specimen figure 21

Figure 21 schematics of SEM

Mathematically, magnification is give by the relation shown bellow
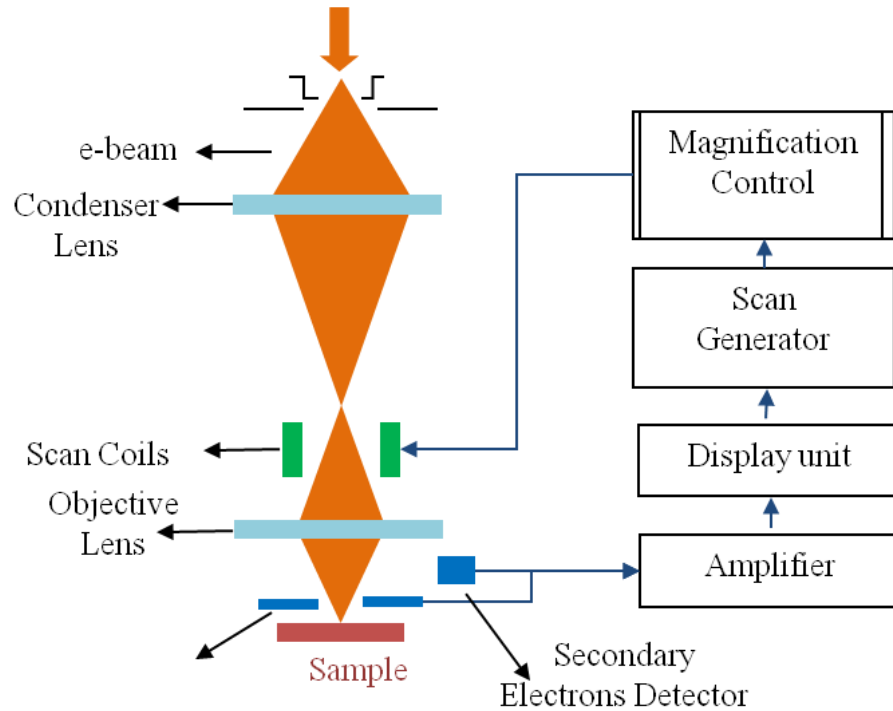
$$M = Lmon/Lspec.$$

Where Lmon is the scan length of monitor, while lspec is the scan length of the specimen. Thus scanning smaller area of the sample gives high magnification.

4.1.4. Image quality

The SEM imaging consists of measurement various types of events which are controlled at the detector[27]. The signal measurement is the measurement of the amount or quantity of electrons at the detector, while presence of noise can decrease the quality of image, thus the image quality is defined as the ratio of the signal to noise i.e. S/N.

The ratio indicates that increased I the average number of electrons can improve the quality because with increasing electrons, the fluctuations or noise becomes lesser contributor in the formula.

The contrast is defined as the ratio of the difference of signals detected at two points divided by one of them i.e.

$$Contrast=(S2 – S1)/ S2$$

Where s2 and s1 are the signals detected at two arbitrary points, and S2 >S1, that means contrast can always be positive ranges from 0 to 1.

4.1.5. Signals and imaging modes in the SEM

Secondary electrons and back scattered electrons are the primary signals carriers in SEM[26]. These differ in their energies. Secondary electrons have comparatively low energy around 5Ev, while back scattered electrons have high energies, usually equal or comparable to the energies of incident electrons that is in the rage of several thousand electron volts[25].

4.1.6. Compositional contrast

This is also called atomic number contrast which occurs due the difference in the atomic number at the respective areas, due to which the intensity of the signal from those areas differs. High atomic areas appear bright as compared to low atomic areas. Mathematically the atomic number contrast is give by

$$C = (n1-n2)/ n2$$

Where n1 and n2 are the back scattered coefficients of the two regions. The more is the difference in the atomic numbers, the more is the contrast and vice versa.

4.1.7. Topographic contrast

This includes all those effects which play role in the imaging of the shape and morphology of the samples. Trajectories and number of secondary electrons and

back scattered electrons depends on the angle of incidence between the specimen's surface and the beam, due to which topographic contrast is developed. The angle of incidence depends on the specimen surface. When the beam strikes at each point, the detector gets direct information on the inclination as due to secondary and back scattered electrons. Finally the interpretation and analysis of image does not require the information regarding the mechanism of image formation.

4.2. Defect in SEM imaging

Several defects are associated with the imaging of SEM:-

1. **Contamination**:- this includes the deposition of some unwanted or external molecules on the specimen surface[27]. They may be the carbonaceous materials which are the derivatives the hydrocarbons. Due to this deposition, the scattered electron coefficient changes thus contrast is developed. Imaging at low magnification, and then gradually increasing the magnification can reduce this effect. Mainly, the beam is contaminated by hydrocarbon molecules, which sometimes affect the signals even at high magnification. The important step to reduce contamination is to increase the vacuum inside the chamber. Some anti-contamination devices can also be installed near the specimen, which can make the system cool. Also it is reduced by exposing the specimen to ultraviolet light before imaging.

2. **Charging**:- Not all the incident electrons are scattered back from the specimen, but many of them penetrate into the specimen and remain there as their kinetic energy is reduced. Now if the specimen is not properly ground, these impart a net charge to the sample, due to which the specimen's surface potential rises. Usually, insulator materials undergo this charging effect, because electron does not flow properly, so they cannot reach the ground. The field line of the detector get disturbs when there occurs a local charging and surface potential is altered. These all affect the collection of secondary electrons. Also due this local charging, voltage contrast is developed, and the potential distribution is imaged. Some areas appear darker and some areas appear bright due to localized opposite charges.

4.3. Sample requirements

The SEM is operated under high vacuum (approx 10-5mbar) thus the specimen must be compatible to such high vacuum. This implies that liquids and materials containing liquids cannot be directly tested, and also the volatile compounds and fine powders are difficult to study. To avoid the contamination of the chambers, these materials are tightly fixed to the sample holder. In case of nonconductive

samples, they must be attached to some conductive holders and also a thin conductive film is coated by sputtering. Coating materials include gold, platinum, their alloys and carbon. [27]

4.4. Results

SEM was done to study the surface morphology and dimensionality of the nanorods. The following images from a to e are the SEM images of various samples grown on ITO substrate fig (3). The images show a uniform density, homogeneity, smoothness and vertically alignment along the c-axis.
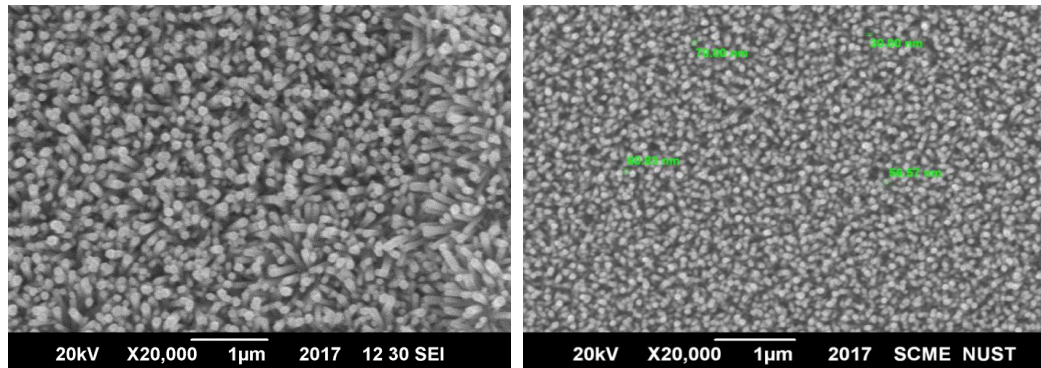
Figure 22 SEM images of inverted sample at 120°C for 3.5 hrs, and slanted at 120°C FOR 3.5 Hrs
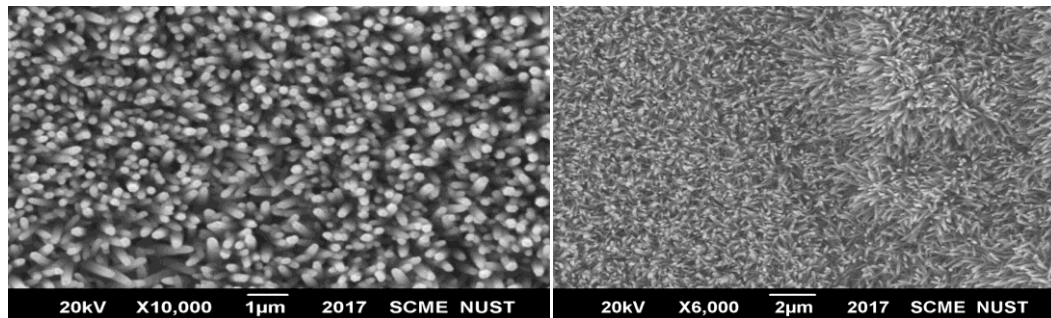
Figure 23 SEM images of inverted at 100°C for 2,5 hrs, andslanted at 140°C FOR 4.5 Hrs
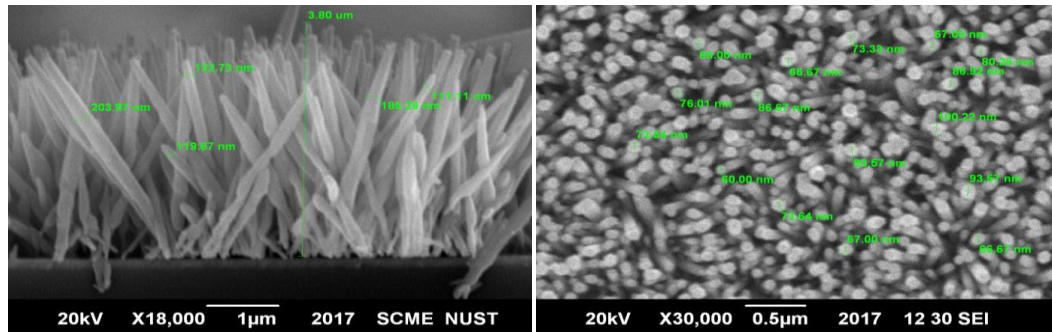
Figure 24 CBD groth at 90°C   for 3 hours, and edge view of slanted at 120°C   for 3.5 hrs

The distribution is uniform with an average diameter of 120.2943 ± 8.0147 nm. The length calculate by the imageJ is 2.8691± 0.1434 micrometer. The average aspect ratio calculate is 24, which satisfies our requirements. It is clear from the images that the ZnO nanorods have rod like hexagonal structure, which also corresponds with the XRD results.

4.5. X-RAY diffraction and Crystallography

What are X-Rays?

X-Rays are basically electromagnetic waves which have high frequency and a very short wavelength, ultimately having high energies fig 27. Due to the aforementioned properties X-rays have the ability to penetrate or pass through materials.
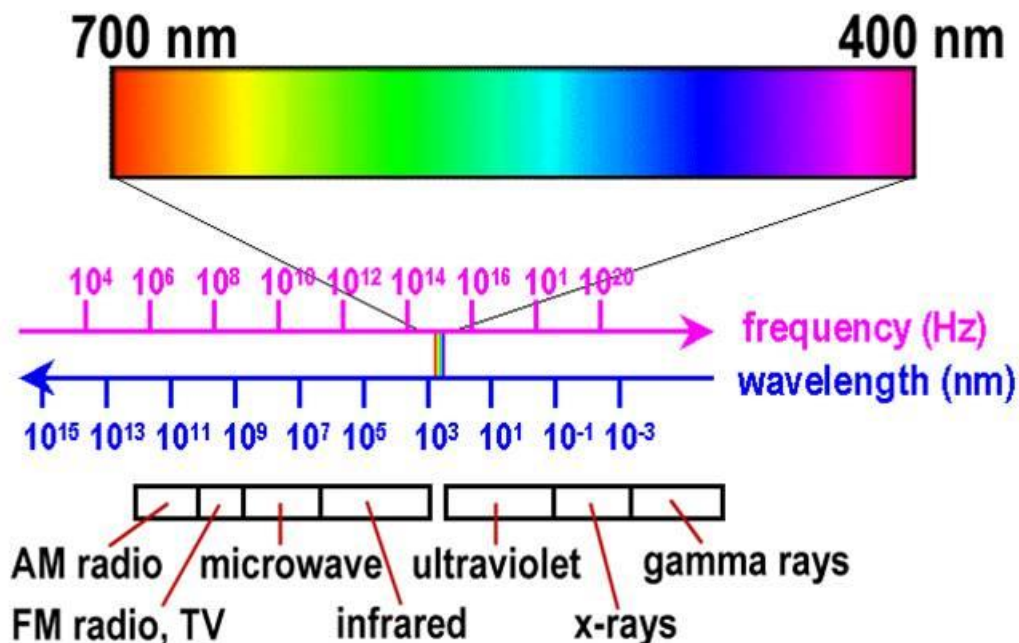
Figure 25 electromagnetic spectrum

What is crystallography?

The investigation and determination of the crystal structure of any substance using x-ray diffraction technique is called crystallography of x-ray crystallography.

4.5.1. Properties of X-RAYS

Properties of x-rays can be divided into four types i.e. physical, chemical, and biological and physiochemical.

4.5.2. Physical properties

1. X-rays are electromagnetic in nature, does not require any medium to propagate, and their wavelength ranges from 0.5 Å to 10 Å.

2. X rays always travel in straight path in free space

3. Their speed is equivalent to that of visible light i.e. 186000 miles/second

4. They cannot be seen by naked eyes, cannot be heard and they don't have any smell. 5. One cannot focus them on a single point

6. Phenomena like refraction, diffraction and interference are shown by xrays.

7. In the presence of magnetic or electric field, the cannot show deflection, refraction and reflection

8. Electric field id developed at right angle to their path, and produce magnetic field perpendicular to both the path and the electric field

9. They penetrate into gases, liquids and solids, but the penetration depth depends on the wavelength, intensity and quality of x-rays

10. X-rays are also absorbed by some materials which depend on the energy of the x rays and the atomic structure of the material

11. While passing through the material they interact with it and cause ionization.

12. Few substance emit visible light when x-rays fall on them, this is called fluorescence.

13. They also heat up the material, and they have the property of scattering, absorption and attenuation.

4.5.3. Chemical properties

1. Many substance show a change in color when x-rays are passed through it. For example Methylene blue changes to bleached

2. In case of solution, x-rays produce OH radical which react with the solute and thus chemical changes occur

3. Enzymes loss their fermenting power when gets exposed to x-rays

4.5.4. Biological properties

1. Malignant lesion or cancerous patients are treated by using the excitation property of x-rays

2. They also used as bactericidal or germicidal

4.5.5. Physiological properties

1. X-rays have the ability to produce an image on the photographic films, even of the internal parts

4.6. Working principle of X-RAYS

When a crystalline substance is exposed to X-rays it acts like a three dimensional diffraction grating for them. Constructive interference of the monochromatic xrays is the base of the x-ray diffraction crystallography. X-rays are produced in the cathode ray tube, and then they are filtered to have monochromatic rays, concentrate them and then directed to the specimen. Now if the **Bragg's law ($n\lambda=2d \sin \theta$)** is satisfied, constructive interference is experienced. $n\lambda=2d \sin \theta$ This relates the lattice spacing, diffraction angle and the wavelength of the xray used. Detector detects the diffracted x-rays, processor processes them and they are counted. Scanning the sample in the 2 theta range, all possible planes show diffraction, and conversion of these peaks into lattice spacing give information about the sample material i.e. by comparing the d spacing with the reference patterns.
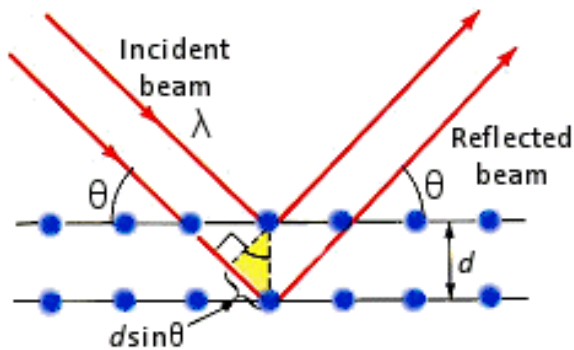

Figure 26 diffraction of light

The most common target element to generate X- rays is copper. Mostly copper Kα radiation with the wavelength of 1.5418A is used. The generated X-rays are directed towards the sample, and the reflected intensity is recorded. When Bragg's law is satisfied, constructive interference occurs and the intensity of peaks is observed.
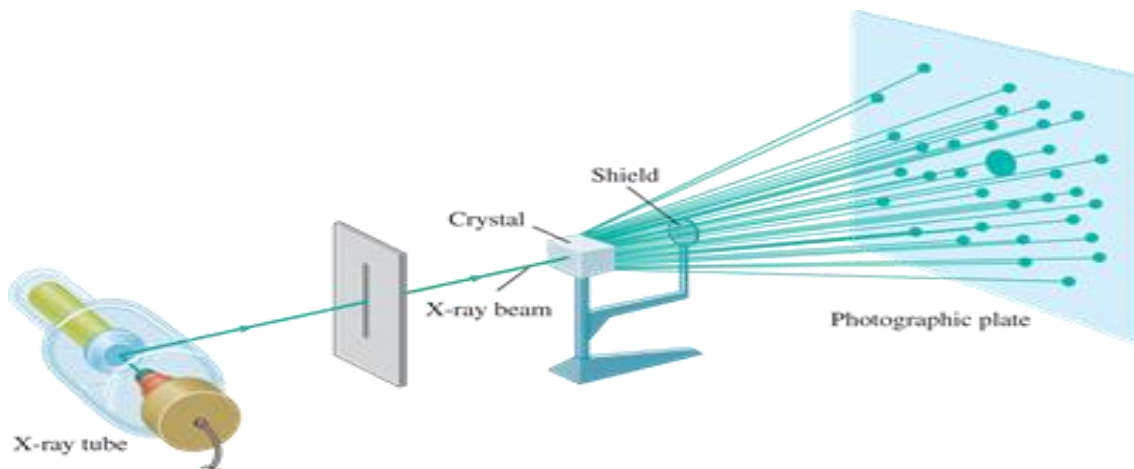
Figure 27 schematics of X-Ray diffraction

Image source: https://sites.google.com/a/hartdistrict.org/ms-smith/home/modern-solid-materials/chapter-11-intermolecular-forces-and-liquids-and-solids/11-5-x-ray-diffraction-by-crystals

4.7. Results

The crystal structure of ZnO nanorods was studied by using XRD. Figure 29 shows the plots inverted sample and tilted sample. The plots indicate that they correspond to polycrystalline hexagonal ZnO nanorods, by showing the peaks at 32°, 34.4° and 36.5°, which exactly match with the peak positions of ZnO. The lattice parameters are 0.32498 nm, 0.32498 nm and 0.52066 nm respectively. In case of tilted sample at 120°C, all peaks are indexed to ZnO, while in inverted sample, extra peaks at 30° and 52 ° belong to the substrate i.e. as the XRD plot of ITO is shown below. The reason to observe the peaks of ITO is that the x-rays have high penetrating power which is upto 3mm, so they they reached ITO too. The reference code against which the sample was compared is 00-036-1451. In figure 30 both the plots reveal that the three major peaks belong to ZnO, while the extra peaks are indexed for ITO
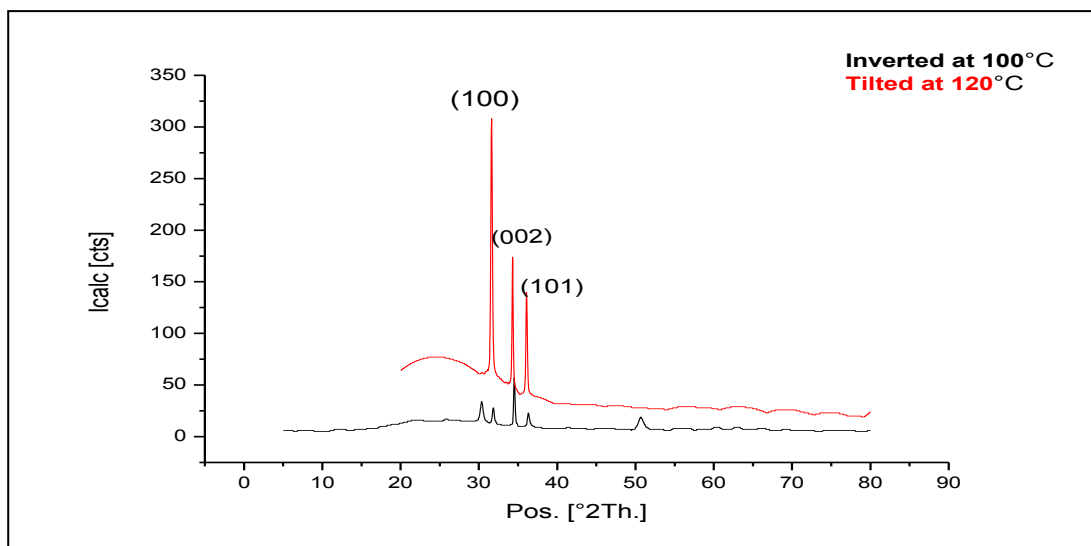
Figure 28 :-XRD plots of inverted sample at 100°C for 2.5 hrs and tilted sample at 120°C for 3.5 hrs

Crystallographic parameters

Reference code: 00-036-1451
Crystal system: Hexagonal
Mineral name: Zincite, syn
Space group: P63mc
Space group number: 186

a (Å):   3.2498
b (Å):   3.2498
c (Å):   5.2066
Alpha (°): 90.0000
Beta (°):   90.0000
Gamma (°):   120.0000

Volume of cell (10^6 pm^3):   47.62
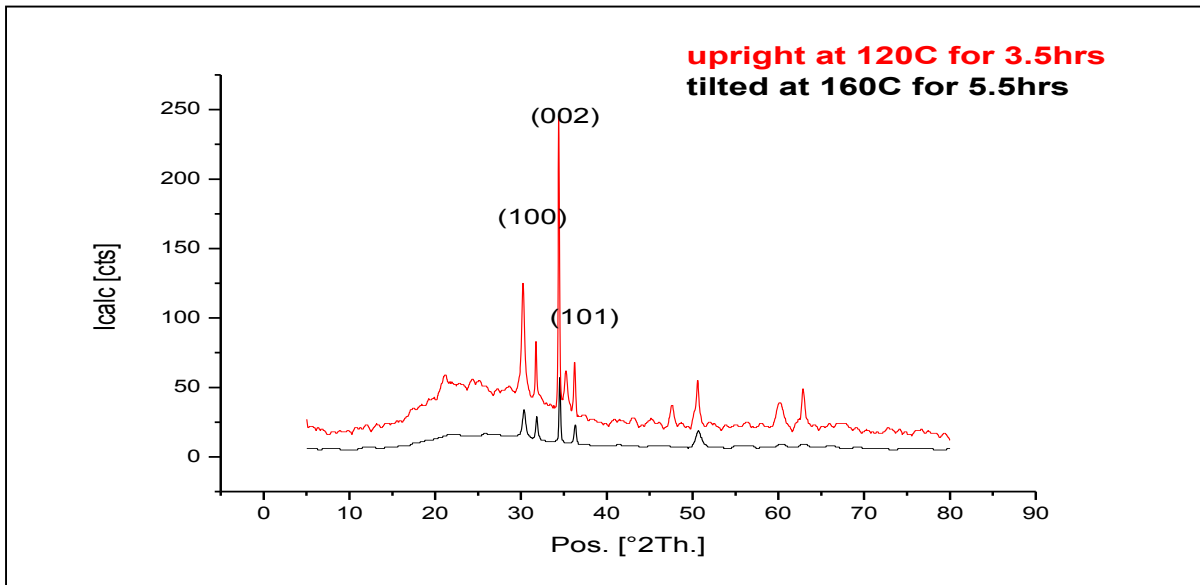
Figure 29 XRD plots of sideways placed at 120°C for 3.5 hrs and slanted at 140°C FOR 4.5 hrs
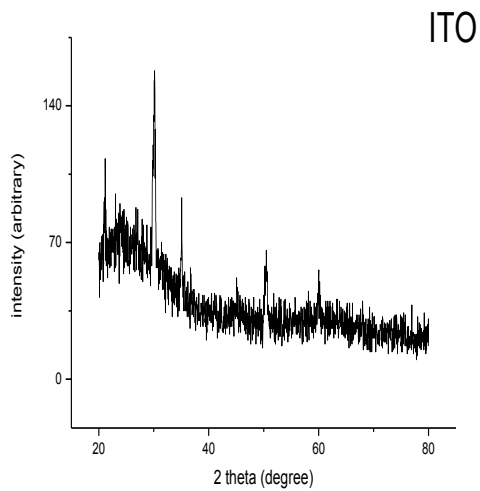
Figure 30 XRD plot for the sidewas placed at 120°C FOR 3.5hrs

In figure 31, little asymmetrical peaks are seen. The reasons to observe these peaks may be the presence of defects and their uneven distribution, like any impurity or and interstitial which actually alters the lattice spacing. Also presence of stresses can lead to have the asymmetric peaks.

4.8.IV characteristics

As ZnO is an n-type semiconductor, and the gas sensing properties are due to its surface resistance. In air, oxygen is absorbed or chemisorbed[28] on the surface and it acts as trap while capturing electrons from the conduction band,[29] due to its high electro negativity. As a result, depletion region produces on the surface. Now it

45

depends on the gas to be sense, if it is oxidizing it will decrease the conductivity of increase the resistivity. Similarly, in case of reducing gas, the resistivity will decrease and conductivity will be enhanced

We studied the IV characteristics on the electrochemical station. The IV characteristics of ZnO were studied in vacuum, in open air, in nitrogen, in ethanol (also in UV), and also when the substrate was exposed to methane. The area of the substrate or sample was 1.5cm2 i.e. (1x1.5) cm2 .
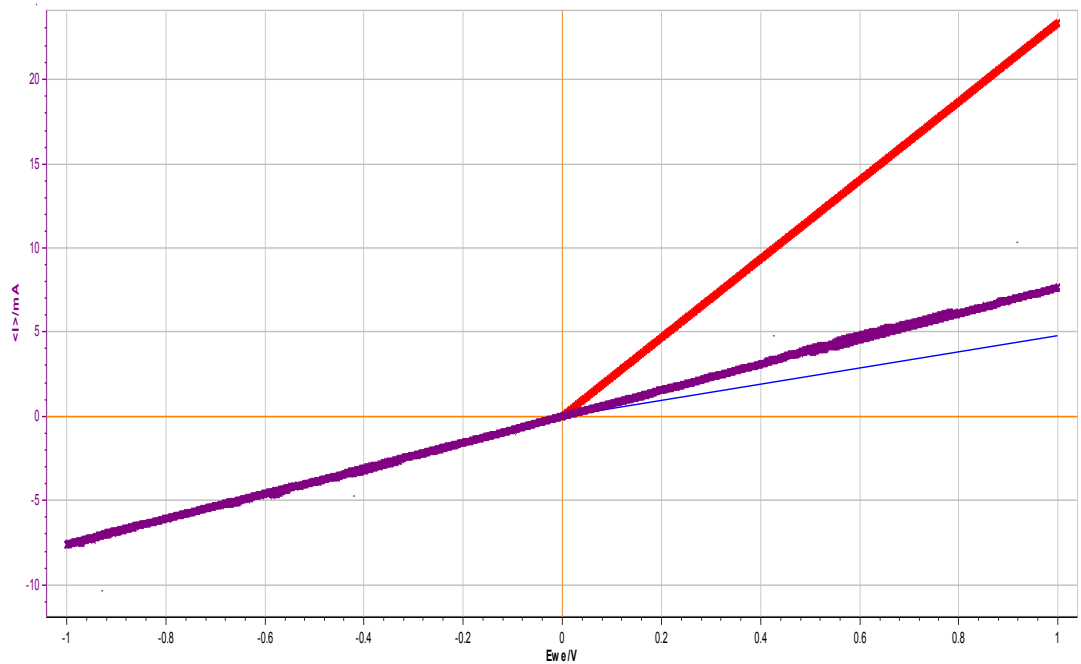
Figure 31 IV plots ZnO in air, ZnO in UV(2 inch apart), ZnO in UV (4 inch apart) and pure ITO

The IV plots in the figure xx show that their slops change as the medium is changed, in case of pure ITO the conductivity is very high as it is obvious from the slope. It is because the ITO is conductor. But when the ITO substrate having ZnO nanorods on it is exposed to air, the conductivity decreses or its resistance increases, because the oxygen from the air gets adsorbed on the surface of ZnO and it captures the conduction electrons of the ZnO, due to which the charge carriers decreases in amount. Hence the resistance increases.

When the sensor was exposed to UV light, the conductivity increased because UV light can excite the charge carriers. Further when the distance between the UV source and the sensor was decreased, the conductivity further increased that indicates that the high intense UV light increases the sensitivity of the sensor.

The UV detection mechanism depends on the intrinsic defects like oxygen vacancies and zinc interstitials. It is already mentioned that the chemisorbed oxygen molecules on the surface confine the free electrons of the ZnO sensor.

$$O2\ g + e\text{-} \rightarrow O2 - ads.\ (1)$$
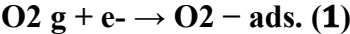
When uv light of energy greater than the band gape of ZnO is incidented, electron-holepairs are formed. Adsorbed oxygen combine with the hoe to form oxygen molecule and then desorbed, decreasing in the width of deplition region, thus increasing the conductivity.

$$h + h\vartheta + O2 - ads. \rightarrow O2\ (2)$$
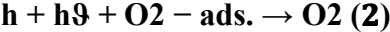
After the UV light, the oxygen gets reabsorbed until the equilibrium is regained. This is slow process which actually increases the relaxation time constant for the device.
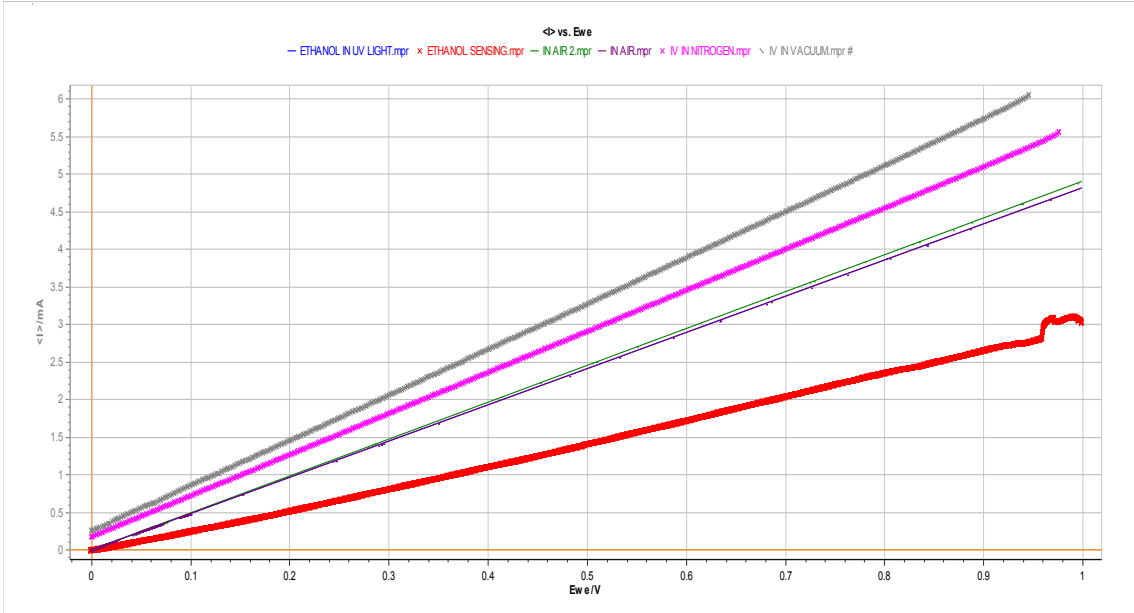
Figure 32 IV characteristic in vacuum, air, nitrogen, ethanol and ethanol in UV light

Figure.32 shows the IV plots for different mediums including vacuum, nitrogen, air, ethanol and ethanol in the presence of UV light. Resistance of the sensor in vacuum is very low as shown by the slope of the plot. When it was exposed to nitrogen the resistance increased. Further in ambient air resistance increased. In case of ethanol, the conductivity decreased but when we exposed the sensor to UV light, the conductivity increased, hence it was concluded that the UV increases the sensitivity or the conductivity of the ZnO gas sensor by exciting the electron.

Table 3: shows the resistances of the sensor for the mentioned medium

Medium	Resistance
Vacuum	150 Ohm
nitrogen	175 Ohm
Air	208 Ohm
Ethanol	322 Ohm
Ethanol in UV	212 Ohm

4.8.1. Methane sensing

Methane is one the reducing gas, hence its increases the conductivity of ZnO nanorods. The adsorbed oxygen increases the surface resistance of the sensor by capturing the conduction electrons. Methane actually reacts with the adsorbed oxygen and the trapped electrons are sent back to the conduction band [30] due to which the resistance decreases and the conductivity increases. The entire reactions are shown as

$$O_2(gas) \rightarrow O_2(ads) \; O_2(ads) + e^- \rightarrow O_2^-(ads)$$

$$O_2^- (ads) + e^- \rightarrow 2O^-(ads) \; O\text{-}(ads) + e^- \rightarrow O_2^-(ads)$$

$$CH_4(gas) + 2O_2^-(ads) \rightarrow CO_2(gas) + 2H_2O(gas) + 2e^-$$

$$CH_4(gas) + 4O^-(ads) \rightarrow CO_2(gas) + 2H_2O(gas) + 4e^-$$

$$CH_4(gas) + 4O_2^-(ads) \rightarrow CO_2(gas) + 2H_2O(gas) + 8e^-$$
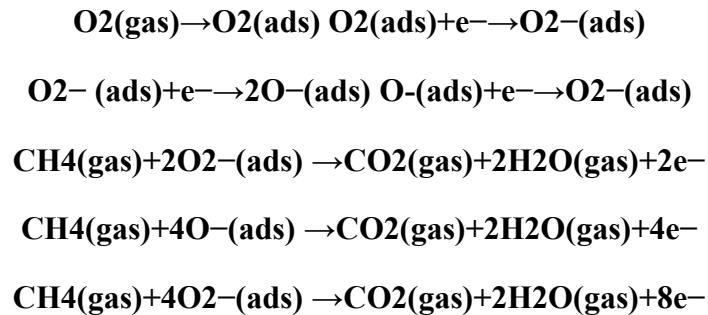
The IV plots shown in the figure 34 for various concentrations of methane show that the resistance changes with change in concentration. The resistance gets decreased as the concentration is increased i.e. the conductivity increases with increase in the methane concentration. The resistance and the sensitivity values for various concentrations are shown in the table xxx
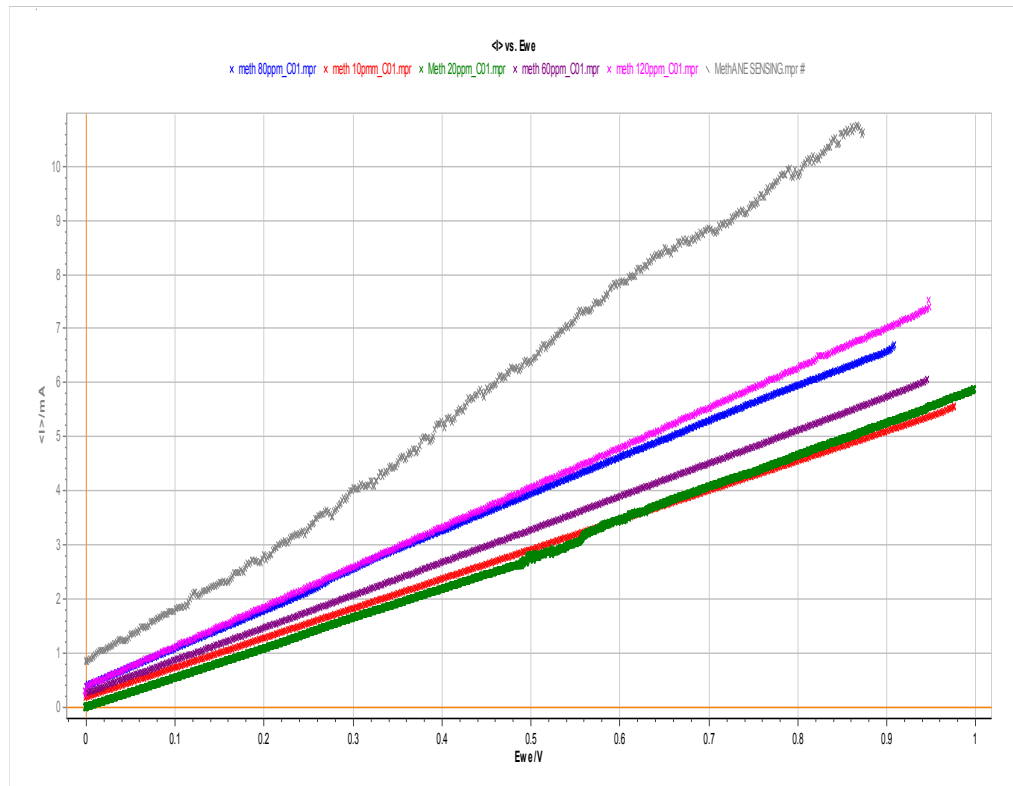
Figure 33 IV characteriscs for methane sensing at 10ppm, 30ppm, 60ppm, 90ppm, 120ppm and 150ppm

Table 4. Resistance

Concentration of methane	Resistance	Sensitivity R_{air}/R_{gas}
10 ppm	178 Ohm	1.17
30 ppm	169 Ohm	1.22
60 ppm	138 Ohm	1.51
90 ppm	134 Ohm	1.55
120 ppm	126 Ohm	1.64
150 ppm	82 Ohm	2.53

5.Chapter 5: Conclusions

The experimentation in both phases produced results, revealed via the characterization techniques discussed above, that can be concluded as follows:

1-Spin coating is a more effective method for seed layer deposition

2-Hydrothermal reaction provides the best aspect ratio and alignment of nanorods at the following conditions:

Growth Time:	3.5 hrs
Growth Temperature:	120° C
Substrate Orientation:	Tilted

3-CBD provides better uniformity than the hydrothermal method

4-Hydrothermal method provides better control and hence a better aspect ratio of the nanorods.

5-ZnO's conductivity varies when in exposure to UV light

6-ZnO's conductivity is sensitive to gas molecules' interaction with the surface

7-The sensitivity of ZnO nanorod conductivity tends to amplify under the exposure of UV light in one experiment

All of these conclusions verify that the objectives of our final year project were successfully achieved.

Future directions

The project can be taken into the following directions in terms of research as well as commercialization:

Research Directions:

-Growth of core-shell nanorods and comparison of their gas detection detection properties with the work of this thesis as a benchmark.
-Deposition of nanoparticles on the rods and evaluating the effects on gas detection properties, again with this work as reference for values.
-Designing a three-electrode sensor instead of the current two-electrode configuration, in order to perform Cyclic Voltametry tests.

Commercialization Directions:

-Collaborating with students from SEECS to develop the required circuit, proposed in FICS 2017, for developing a functional real-time sensor.
-Tuning the current configuration to achieve detection of gases required in oil and gas industries to establish a local market (current sensors are being imported).

References

1.   Dewei Chu, Y.M., Tatsuki Ohji, and Kazumi Kato, *Formation and Photocatalytic Application of ZnO Nanotubes Using Aqueous Solution.* 2009: p. 1-5.
2.   Wang, Z.L., *Zinc oxide nanostructures: growth, properties and applications.* JOURNAL OF PHYSICS: CONDENSED MATTER 2004: p. 1-30.
3.   Pearton, C.J.S., ed. *Zinc Oxide Bulk, Thin Films and Nanostructures*. 2006. 600.
4.   Hahn, A.U.a.Y.-B., ed. *Metal Oxide Nanostructures and Their Applications*. Vol. 5. 2010, American Scientific Publishers 1-36.
5.   Cui, J., *Zinc oxide nanowires.* M A T E R I A L S C H A R A C T E R I Z A T I O N, 2011: p. 1-11.
6.   *<Dieter_Kohl_2001_J._Phys._D%3A_Appl._Phys._34_201.pdf>.*
7.   Kołodziejczak-Radzimska, A. and T. Jesionowski, *Zinc Oxide—From Synthesis to Application: A Review.* Materials, 2014. **7**(4): p. 2833-2881.
8.   Materials, A., *Zinc Oxide – Properties, Applications and the Future for ZnO*. 2011.
9.   Hadis Morkoc, U.O., *Zinc Oxide: Fundamentals, Materials and Device Technology*. 2009.
10.   Walle, A.J.a.C.G.V.d., *Fundamentals of zinc oxide as a semiconductor.* 2009: p. 1-29.
11.   Tigli, J.L.G.O., *Zinc oxide nanostructures: from growth to application.* 2012: p. 1-13.
12.   Qin, Q.P.a.Y., *ZnO Nanowires and Their Application for Solar Cells* in *Nanowires-Implementations and Applications*.
13.   Steinhauer, S., *Gas Sensing Properties of Metal Oxide Nanowires and their CMOS Integration*. 2014, Technischen Universita¨t Wien
14.   C. X. Xu, G.P.Z., X. Li, Y. Yang, S. T. Tan, X. W. Sun, C. Lincoln, and T. A. Smith, *Growth and spectral analysis of ZnO nanotubes.* : Journal of Applied Physics 2008: p. 1-6.
15.   MUKHOPADHYAY2, P.M.a.A.K., *ZnO thin film as methane sensor.* BULLETIN OF THE POLISH ACADEMY OF SCIENCES TECHNICAL SCIENCES, 2007. **55**: p. 1-5.
16.   J.N. Hasnidawani, H.N.A., H. Norita, N.N. Bonnia, S.Ratim and E.S. Ali, *Synthesis of ZnO Nanostructures Using Sol-Gel Method.* Procedia Chemistry, 2016. **19**: p. 211-216.
17.   Serdar AYDIN, G.T., Mehmet YILMAZ, Mehmet ERTUĞRUL *Fabrication of ZnO nanorods by simplified spray pyrolysis* Bitlis Eren University Journal of Science and Technology 2011: p. 1-3.
18.   M. Verde , M.P., A.C. Caballero , M. Villegas , B. Ferrari *Electrophoretic Deposition of Transparent ZnO Thin Films from Highly Stabilized Colloidal Suspensions* p. 1-7.
19.   Akram, M.A., S. Javed, and M. Mujahid, *Synthesis and Surface Modification of ZnO Nanorods Arrays.* Advanced Materials Research, 2015. **1119**: p. 49-53.
20.   Di Liu, Y.L., Ruilong Zong, Xiaojuan Bai, Yongfa Zhu, *Controlled synthesis of 1D ZnO nanostructures via hydrothermal process.* Materials research Bulletin, 2014. **49**: p. 665-671.
21.   Yangyang Zhang, M.K.R., Elias K. Stefanakos, and D. Yogi Goswami, *Synthesis, Characterization, and Applications of ZnO Nanowires.* Journal of Nanomaterials, 2012. **2012**: p. 22.

22.	Qi-Hui-Wu, *ZnO nanostructures prepared using a vapour transport method.* journal of experimental nanoscience, 2013. **10**: p. 161-166.

23.	Hiroyuki Nishinaka, T.K.a.S.F., *Growth of ZnO Nanostructures by Using Ultrasonic Spray Chemical Vapor Deposition with a Au Catalyst.* Journal of the Korean Physical Society, 2007. **53**: p. 3025-3028.

24.	M.K. Tsaia, C.C.H., Y.C. Leea,n, C.S. Yangb, H.C. Yub, J.W. Leec, S.Y. Hud, C.H. Chene, *A study on morphology control and optical properties of ZnO nanorods synthesized by microwave heating.* Journal of Luminescence, 2011. **132**: p. 226-230.

25.	Vernon-Parry, K.D., *Scanning electron microscopy: an introduction.* III-Vs Review, 2000. **13**(4): p. 40-44.

26.	A. Bogner, P.-H.J., G. Thollet, D. Basset, C. Gauthier, *A history of scanning electron microscopy developments: Towards ''wet-STEM'' imaging.* 2007: p. 390-401.

27.	*<sem-intro.pdf>.*

28.	Sarkar, A., et al., *Responsivity optimization of methane gas sensor through the modification of hexagonal nanorod and reduction of defect states.* Superlattices and Microstructures, 2017. **102**: p. 459-469.

29.	Wang, Z.L., *Nanostructures of zinc oxide.* Materials Today, 2004. **7**(6): p. 26-33.

30.	Zhou, Q., et al., *Hydrothermal Synthesis of Various Hierarchical ZnO Nanostructures and Their Methane Sensing Properties.* Sensors, 2013. **13**(5): p. 6171-6182.